Title

A high-quality reference genome for the Ural Owl (*Strix uralensis*) enables investigations of cell cultures as a genomic resource for endangered species

Authors

Ioannis Chrysostomakis[1], Annika Mozer[1], Camilla Bruno Di-Nizo[1], Dominik Fischer[2], Nafiseh Sargheini[3], Laura von der Mark[1], Bruno Huettel[3], Jonas J. Ast rin[1], Till Töpfer[1], Astrid Böhne[1]

Affiliations

[1]Leibniz Institute for the Analysis of Biodiversity Change, Museum Koenig Bonn, Adenauerallee 127, 53113 Bonn, Germany

[2]Zoo Wuppertal, Wuppertal, Germany

[3]Max Planck Genome-Centre Cologne, Max Planck Institute for Plant Breeding Research, Carl-von-Linne-Weg 10, 50829 Cologne, Germany

Keywords

Strix uralensis, Strigidae, karyotyping, genome sequence, genome annotation, cell culture, SNP, variant

Abstract

We generated a reference genome for the Ural Owl (*Strix uralensis*) based on high-fidelity (HiFi) long reads and chromosome conformation capture (Hi-C) data. The primary assembly had a size of 1.38 gigabase pairs (Gb), while the alternative assembly (i.e., the second haplotype) had a size of 1.3 Gb. The corresponding N50 was 90.1 Mb for the primary assembly and 17.0 Mb for the alternate assembly. The primary assembly achieved a compleasm BUSCO completeness of 99.94%, indicative of a high-quality genome. In addition, cell culture of progressive passages was evaluated as a tool for genetic resources. To this aim, a cell culture of the same Ural Owl individual was established from skin tissue. At passages 5 and 10, cells were harvested and investigated for possible nucleotide variants by analysing the karyotype and single nucleotide polymorphisms (SNPs) to investigate the effect of cell culture on mutation. Karyotyping confirmed the number of chromosomes and no large variants were observed, while SNP analysis revealed a minor presence of short variants over cell passages. The established reference genome is a valuable resource for ongoing conservation efforts but also generally for avian genomics research. Cell culture, on the other hand, requires more research to determine if progressive passages can be safely used in genomic research.

Introduction

High-quality reference genomes are rapidly becoming available for many branches of the tree of life (https://www.earthbiogenome.org). These data are now increasingly used for comparative genomic studies on large evolutionary timescales trying to link phenotypes to genotypes. However, even in genomically and traditionally well-studied groups such as birds, several lineages still lack high-quality reference genome assemblies that would allow for detailed studies of genome evolution.

Typical avian karyotypes are composed of macro- and microchromosomes (but see (Ellegren, 2010; Rebholz et al., 1993)). Compared to macrochromosomes, which are typically between 30 and 250 mega base pairs (Mb) in size, microchromosomes have an average size of 12 Mb, although microchromosomes as small as 3.4 Mb have been observed (Burt, 2002; Pichugin et al., 2001). Despite recent efforts to characterise avian genomes and understand their karyotype evolution, less than 10% of all known species have a characterized karyotype (Degrandi et al., 2020). The diploid number of about half of these varies between 78 to 82 chromosome (Ellegren, 2010). Regarding the family Strigiformes (owls), karyotype information is available for 13% of species (Degrandi et al., 2020). Interestingly, microchromosomes encode half of the genes in birds, although they account for only about a quarter of the genome (Burt, 2002; Smith et al., 2000). Moreover, another study indicates that the mutation rate of microchromosomes is significantly higher than that of macrochromosomes (Axelsson et al., 2005). Therefore, the karyotypes and especially the microchromosomes seem to deserve more cytogenetic and molecular studies.

To this aim, we here provide a first high-quality reference genome for the Ural Owl (*Strix uralensis*). This species is one of the largest Eurasian owls, inhabiting the Palaearctic lowlands up to the treeline, mainly in the taiga forest belt over a large uninterrupted range from Scandinavia through Siberia to Sakhalin and the Japanese islands. It also occurs in geographically isolated, mixed and deciduous forests of southeastern and central Europe

(southern Germany, Czech Republic, Austria, Slovenia and Poland; partly supported by reintroductions). So far 11 subspecies have been described from its vast distribution based on differences in size and colouration (Cramp, 1989); although not all of these have been widely accepted (Able, 2000). Furthermore, the molecular data at hand (i.e., mitochondrial and nuclear marker genes) do not support morphology-based taxonomic distinctions (Hausknecht et al., 2014). Interestingly, in the populations from the Carpathians to the Dinaric Alps (ssp. *macroura*), melanistic (i.e., very dark or almost black) individuals are common (Vrezec, 2009).

Ural Owls are nocturnal hunters of small mammals and birds and usually stay in their territories throughout the year (Able, 2000; Cramp, 1989). As the Ural Owl is sedentary and nests in hollow stumps or tree holes (König & Weick, 2009; Mikkola & Willis, 1983), it is affected by ecosystem degradation (IUCN, 2021). Nesting sites have been reduced by intensive logging activities, agricultural use, and forestry management (IUCN, 2021; König & Weick, 2009). Direct persecution mainly drove the extinction of *S. uralensis* in Austria, southern Germany, and the Czech Republic in the last century (Kopij, 2011; Scherzinger, 2006; Soorae, 2011). Successful reintroductions have taken place in these countries (e.g. (Kopij, 2011; Scherzinger, 2006; Soorae, 2011)). A key to the success of thereintroductions has been the provision of nest boxes (Soorae, 2011). These central European reintroductions have restored gene flow between the remaining Alpine and European populations (Hausknecht et al., 2014; Scope et al., 2016). The Ural Owl will likely further be affected by climate change, potentially shifting its range to more northern regions (Huntley et al., 2007) and altering breeding times (Lehikoinen et al., 2011).

Cryobanking, in a strict sense the preservation of viable cells and tissues at ultracold temperatures (typically using liquid nitrogen), has been considered of paramount importance in preserving the genetic variability of species, especially the ones facing population decline, to ensure population health and persistence (Mooney et al., 2023; Ryder & Onuma, 2018). Although some instances have been reported where long-term cell culture generated genetic instability and heteroploidy (Freshney, 2010; Hughes et al., 2007), it is still unclear how far-

spread such a phenomenon is and at which stage of cell cultivation it occurs.

Herein, we generated a reference genome for the Ural Owl as a genomic resource to facilitate further research on this species and on Strigidae more generally. We assess the genome assembly quality and provide a first analysis of its gene content in comparison to other avian genomes. As a species of potential conservation concern and as a proof of principle, we further assessed the application of cell culture to produce sufficient DNA in terms of quantity and quality to allow genomics for species with limited biological material. We investigated mutation as a function of passage number (i.e., the transfer of cells from vessel to vessel). To this end, we obtained a cell culture from the same individual that was genome-sequenced, and cultivated the cell lines until passage #10 and subsequently sequenced replicates of passages #5 and #10 (Figure 1).

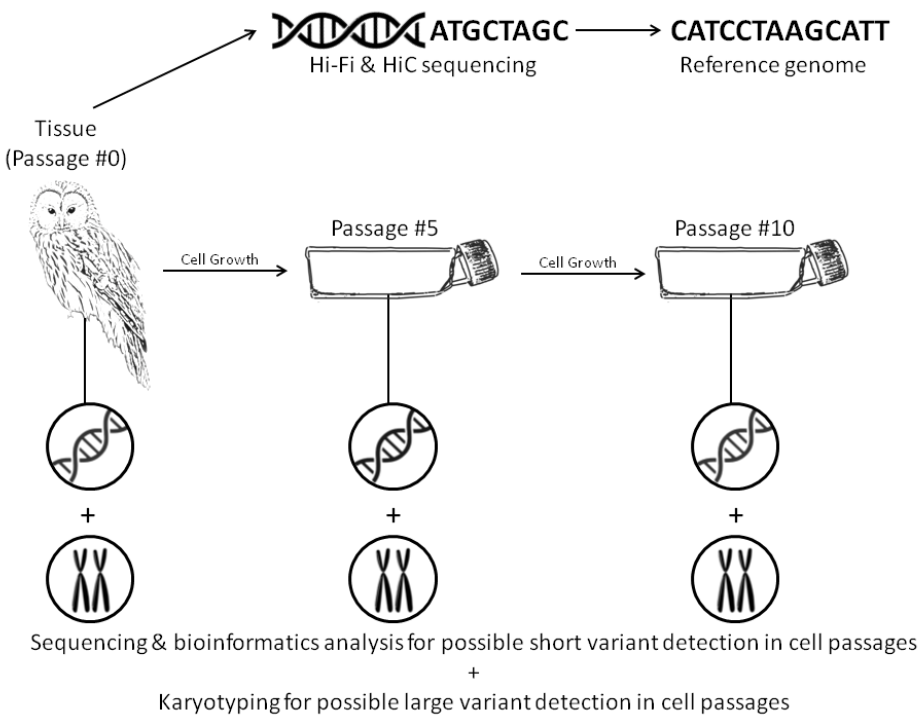

Figure 1: Reference genome and cell passage variant detection workflow. Tissue from a male Ural Owl (*Strix uralensis*) is extracted and sequenced, assembled and annotated to provide a reference genome. Additionally, a cell culture is established from the primary tissue. From passage #0 (primary tissue), passage #5 (three independent replicates) and passage #10 (four independent replicates) cells are harvested for short-read sequencing and karyotyping.

Materials & Methods

Species origin and sampling strategy

Skin and muscle tissue samples from a male individual of *Strix uralensis* (ring ID ZG-14.0-10-0234) were obtained from the Raptor Center & Wildlife Park Hellenthal (Wildfreigehege und Greifvogelstation Hellenthal, Hellenthal, Germany) during necropsy.

Reference genome

Sequencing

DNA was extracted from the skin biopsy (collection ID ZFMK-TIS-50842, stored at LIB Biobank in liquid nitrogen vapor phase) using the Monarch HMW DNA Extraction Kit (NEB, Ipswich, USA). High-molecular weight status was validated by quality control with capillary electrophoresis (Agilent Femto Pulse) and a SPK 3.0 PacBio HiFi library was prepared according to the recommendations by the vendor. Next, HiFi SMRT sequencing was performed on two SMRT cells (8 mio ZMWs) on a PacBio Sequel IIe (Pacific Biosciences, Menlo Park, USA) at the Max-Planck Genome-centre Cologne (MP-GC; Cologne, Germany). Also, a chromatin-capture library was prepared from the same tissue with an Arima-HiC Kit according to the protocol for Mammalian Cell Lines followed by sequencing on an Illumina NextSeq 2000 in paired-end read mode.

Read processing

HiFi data

Contaminant sequences were filtered from the HiFi reads using Kraken2 v2.1.3 (Wood et al., 2019) with the Kraken database kraken2 PlusPFP downloaded in March 2023 and parameters “--confidence 0.51 --use-names”. HiFi read quality was assessed using seqkit v2.8.2 (Shen et al., 2016, 2024) and a k-mer-based approach. K-mers were calculated with Meryl v1.4.1 (Miller et al., 2008) using the parameters “count k=21”, and the counts were converted into a

histogram with the *meryl histogram* command.

To verify the ploidy of the individual, Smudgeplot v0.2.5 (Ranallo-Benavidez et al., 2020) was used. First, k-mers within a specific range (lower-upper), determined with the *smudgeplot.py* cutoff function, were extracted using the meryl *print less-than* command. These filtered k-mers were then processed with *smudgeplot.py hetkmers* to calculate the coverage of unique heterozygous k-mer pairs. The resulting coverage was plotted using smudgeplot_plot.R.

GenomeScope2 v2.0.1 (Ranallo-Benavidez et al., 2020) was used to estimate genome size, heterozygosity, and the homozygous and heterozygous coverage peaks.

HiC data

Adapter removal and quality filtering of the raw Hi-C reads were performed using Fastp v0.23 (Chen et al., 2018) with parameters “--length_required 95, --qualified_quality_phred 20 --adapter_fasta”, with a curated adapter list of the most common adapters used as input.

Error correction was done using *Tadpole* from BBMap v39.01 (https://sourceforge.net/projects/bbmap/), with parameters “k=50, reassemble=t, mode=correct, minprob=0.6, prefilter=1, prehashes=2, and prealloc=t”. To remove contamination from the short, HiC reads, Kraken2 v2.1.3 was used similarly to the HiFi reads but in paired-read mode, with parameter “--paired”.

Initial Genome Assembly

The HiFi reads were used with hifiasm v0.19.5 (Cheng et al., 2021) to generate a phased genome assembly. In order to obtain an optimal, phased genome we tested several hifiasm parameters before choosing the ones that provided us with the assembly of the highest contiguity and completeness with both phased haplotypes having a similar length. We tested all possible combination of different purging level (0, 2, 3), increasing run-time, and number of iterations ("--n-weight 5 --n-perturb 50000 --f-perturb 0.5 -D 10 -N 150 -s 0.2") and explicitly providing the homozygous peak to hifiasm which was estimated by GenomeScope (“--hom-cov 40”) (for more details see Supplementary Table 1).

Genome Scaffolding

The selected haplomes from hifiasm were split at positions containing Ns using *split_fa* from the Purge_Dups package v1.2.6 (Guan et al., 2020). The resulting sequences were mapped to themselves using Minimap2 v2.26 (Li, 2018) with parameters "-x asm5 -DP" and to the HiFi reads using Minimap2 with parameters "-x map-hifi". These mappings were used to remove assembly duplicates with Purge_Dups.

Mitochondrial Genome Detection

To identify and extract the mitochondrial genome, we utilized MitoHiFi v3.2.1 (Allio et al., 2020; Uliano-Silva et al., 2022, 2023), referencing the sequence NC_038218.1 from *Strix uralensis* (isolate C5 mitochondrial genome, complete, https://www.ncbi.nlm.nih.gov/nuccore/NC_038218.1). The most likely scaffold was kept and identified as the mitochondrial chromosome (MT) and all other candidate scaffolds were removed from the assembly.

Assembly Manual Curation

Hi-C reads were aligned to the final assemblies and a Hi-C contact map was created using PretextMap v0.0.2 (https://github.com/sanger-tol/PretextMap). A HiFi coverage track was generated from the aligned HiFi reads using bedtools *genomecov* and integrated into the Pretext map with *PretextGraph.*

Manual curation was performed within PretextView v0.0.2 (https://github.com/sanger-tol/PretextView), where scaffolds were reordered and oriented based on Hi-C interaction frequencies. Following curation, the final assembly scaffolds were processed with AGP tools from the Vertebrate Genomes Project (VGP) using the rapid manual curation protocol (https://gitlab.com/wtsi-grit/rapid-curation/-/tree/main) established by the Darwin Tree of Life consortium (https://www.darwintreeoflife.org/) to create the curated assembly. Scaffold names were further sorted and renamed by size using a combination of seqkit v2.8.2 and SAMtools v1.19.2 (Li et al., 2009).

Genome Quality Control

The completeness of the final curated assembly was assessed using BUSCO v5.8 (Manni et al., 2021) and compleasm v0.2.6 (Huang & Li, 2023) with the aves_odb10 lineage. Assembly contiguity and general assembly metrics were calculated using Quast v5.2.0 (Gurevich et al., 2013).

For k-mer-based analysis, k-mer counts were generated for each assembly using Meryl. These counts were analysed with Merqury v1.3 (Rhie et al., 2020) to estimate assembly completeness and accuracy. The analysis yields Merqury's consensus Quality Value (QV), which is estimated by comparing the read and assembly k-mer counts and then transformed to a log-scaled probability of base-call errors. A higher QV indicates a more accurate assembly. We also obtained a Merqury completeness percent, which reflects the proportions of high-quality HiFi read k-mers present in the assembly.

HiFi reads were mapped to each assembly using Minimap2 v2.26 (Li, 2018) with parameters "-ax map-hifi". Alignment quality and coverage distribution were assessed using Qualimap v2.3 (Okonechnikov et al., 2016).

Potential contamination and quality was also assessed using the blobtoolkit pipeline v. 3.5.4 (Challis et al., 2020) and visualized using the interactive Blobtoolkit viewer in the Galaxy EU server (Afgan et al., 2018).

Genome Annotation

Repeat annotation

Repeat sequences in both assemblies of the *Strix uralensis* reference genome were identified and annotated using a combination of homology-based and *de novo* approaches. Low-complexity repeats and tandem repeats were identified with *DustMasker* from BLAST+ v2.9 (Altschul et al., 1990) and Tandem Repeat Finder v4.10.0 (Benson, 1999), respectively. Transposable elements (TEs) were *de novo* identified with RepeatModeler v2.0.1 (Flynn et

183 al., 2020) to create a species-specific library. This library was combined with the *Strix*-specific
184 repeats library from Dfam 3.1 (Storer et al., 2021) to generate a custom combined repeats
185 library.

186 Repetitive elements in the genome were identified and annotated using this custom library
187 with RepeatMasker v4.1.0 (Tarailo-Graovac & Chen, 2009). Divergence from consensus
188 repeat sequences was estimated using the *calcDivergenceFromAlign.pl* script in
189 RepeatMasker with the *.align* output file. The repeat landscape was plotted with the
190 *createRepeatLandscape.pl* script from RepeatMasker. Output files from DustMasker and
191 Tandem Repeat Finder were converted to GFF3 format using the Perl script *repeat_to_gff.pl*
192 v1.0. RepeatMasker outputs were converted to GFF3 format using RepeatMasker's
193 *rmOutToGFF3.pl* script and edited with a custom Perl command to add unique IDs. Repeat
194 positions were merged using Bedtools v2.29.2 (Quinlan & Hall, 2010) and the genome was
195 softmasked with these identified repeats using Bedtools to prepare for protein-coding gene
196 prediction.

197 Protein-Coding Gene Annotation

198 To perform protein annotation, we created two reference protein sets. Set one contained only
199 the merged proteomes of the following publicly available genomes, downloaded using the
200 NCBI dataset cli v 16.3.0 (O'Leary et al., 2024): *Strix nigrolineata* (GCA_013396715.1), *Gallus*
201 *gallus* (GCF_016699485.2), *Glaucidium brasilianum* (GCA_013399595.1), *Falco peregrinus*
202 (GCF_023634155.1), *Athene cunicularia* (GCF_003259725.1), *Aquila chrysaetos*
203 (GCF_900496995.4) (Mead et al., 2021), *Taeniopygia guttata* (GCF_003957565.2), and *Anas*
204 *platyrhynchos* (GCF_015476345.1).

205 Protein set two was created by merging all proteomes in set one with proteins from the
206 following public and curated databases: i) proteins from the BUSCO v5.4 aves_odb10 dataset,
207 ii) aves proteins from OrthoDB v11 (Kriventseva et al., 2015) were obtained using Tomas
208 Bruna's orthodb-clades pipeline (https://github.com/tomasbruna/orthodb-clades) and iii)

proteomes were also extracted from the UniProt database for the following species: *Calypte anna* (UP000054308), *Steatornis caripensis* (UP000516988), *Cnemophilus loriae* (UP000517678), *Dasyornis broadbenti* (UP000521322), *Corythaixoides concolor* (UP000526942), *Irena cyanogastra* (UP000530962), *Bucco capensis* (UP000534107), *Cephalopterus ornatus* (UP000543364), *Molothrus ater* (UP000553862), *Ptilonorhynchus violaceus* (UP000584880), *Promerops cafer* (UP000587587), *Vidua chalybeata* (UP000634236), and *Urocolius indicus* (UP000654395).

Protein-coding genes in the *Strix uralensis* genome were annotated using a combination of *ab initio*, protein similarity, and transcriptome-based protein prediction models. BRAKER3 v. 3.0.3 (Brůna et al., 2023; Gabriel et al., 2023; Hoff et al., 2016) was run in EP mode using the protein set two described above. GALBA v1.0.11.2 (Brůna et al., 2023) was run using protein set one to annotate genes. The outputs from GALBA and BRAKER3 v3.0.2 were combined using *TSEBRA* from the BRAKER3 package. To ensure high-quality annotations, only the longest gene orthologs for each locus were retained using the *agat_sp_keep_longest_isoform.pl* script from the AGAT package v1.4.1 (Jacques Dainat et al., 2024).

Demographic History of *Strix uralensis*

The demographic history of the Ural Owl was reconstructed using Pairwise Sequentially Markovian Coalescent (PSMC) v0.6.5 as implemented by (Li & Durbin, 2011).

Variants were called per chromosome using a combination of BCFtools v1.21 (Danecek et al., 2021) *mpileup* with parameters “-Q 30 -q 30” and bcftools call using the “-c” option. The resulting VCF file was converted to a consensus fastq format using the *vcfutils.pl* vcf2fq script with parameters “-d 10, -D 60, and -Q 30”.

The PSMC model was run with the following parameters: -N25 -t15 -r5 -p "2+2+25*2+4+6” and 100 bootstraps, a generation time of 3 years (Béziers & Roulin, 2021; Brommer et al., 2002) and an assumed mutation rate of 4.6x10-9 (Fujito et al., 2021; Terhorst et al., 2017).

Owl Genome Synteny

In order to identify the Z sex chromosome within our genome assembly and to assess the synteny of different owl genomes we used the *GetTwoGenomeSyn.pl* built-in script of NGenomeSynt (W. He et al., 2023) with options: "-MappingBin minimap2 -MinLenA 100000 -MinLenB 100000 -NumThreads 5 -MappingPara '-Lx asm5 --eqx -I 200G --MD -N 1'" to estimate chromosome-scale alignments between *Strix aluco*, *Strix uralensis,* and *Bubo scandiacus.* We visualized only contigs that mapped to the curated chromosomes of our genome with an alignment length larger than 1000 bp.

Functional Gene Annotation

Predicted genes were functionally annotated by performing sequence similarity searches against the Swiss-Prot database using *BLASTP* from BLAST v2.13.0+ with default parameters. As with our own genome's annotation, we used *agat_sp_keep_longest_isoform.pl* to only keep the longest isoform of each gene locus from the *Aquila chrysaetos, Gallus gallus, Strix nigrolineata*, *Athene cunicularia, Glaucidium brasilianum, Falco peregrinus,* proteomes of protein set one together with *Tyto alba* (GCA_018691265.1) and *Haliaeetus leucocephalus* (GCA_000737465.1) and used OrthoFinder v2.5.5 (Emms & Kelly, 2019) to estimate orthologous gene families among those species. This analysis identified orthogroups and genes that have undergone expansion or contraction in the Ural Owl, as well as orthogroups unique to this species.

Gene Ontology Term Analysis

Gene Ontology (GO) Term analysis was performed by mapping all Ural Owl genes to the Vertebrate Eggnog database using eggnog mapper v2.1.12 (Cantalapiedra et al., 2021; Huerta-Cepas et al., 2019). Missing GO Terms were filled in with the GO Terms of the previously found Swiss-Prot gene symbols associated with each gene. Next, the genes

258 belonging to gene families unique to the Ural Owl (found with Orthofinder) were analysed by
259 Revigo v1.8.1 (Supek et al., 2011) with default settings and choosing the *Large* subset option.
260 The resulting GO Terms were analysed with Revigo again with default settings and this time
261 with the *Small* subset option. The full *Biological Process* Revigo table was plotted in R v. 4.4.2
262 using an edited version of the Revigo treemap plotting script.

263 Variation analysis over progressive cell passages

264 Cell Culture

265 Primary cells were grown from a skin biopsy of the same individual as used for genome
266 sequencing (collection ID ZFMK-TIS-51054) previously stored at LIB Biobank in liquid
267 nitrogen, following standard protocols. Skin tissues were rapidly thawed, minced into small
268 fragments, and transferred to cell culture flasks. Flasks were incubated at 37°C with 5% CO_2
269 in Fibroblast Growth Basal Medium (FBM; Lonza, Cologne, Germany) supplemented with 20%
270 Fetal Bovine Serum (FBS; Biowest, Nuaillé, France) including antibiotics (100U/mL penicillin
271 and 100g/mL streptomycin; Sigma-Aldrich, St. Louis, United States). Cells were visually
272 inspected in inverted microscope Nikon Eclipse TS2 for contamination and cell media was
273 changed every 2-3 days. After reaching ~80% confluence (determined visually), cells were
274 propagated using 0.125% trypsin solution (Biowest), at subculture ratio 50:50. Cells were
275 harvested for DNA extraction and chromosome analysis at passages #5 (three different
276 replicates) and passage #10 (four different replicates).

277 Chromosome sampling for large variant analysis

278 In order to investigate the stability of the karyotype composition through different passages,
279 chromosome preparations were obtained from cells for passages #5 and #10, according to
280 (Raxworthy, 1987), with modifications. Chromosomes were harvested after treatment with
281 colchicine 0.01% for one hour, followed by hypotonic treatment with 0.075M KCl, and cell
282 fixation in methanol / acetic acid (3:1). Slides were stained with Giemsa 5%. At least 20

283 metaphases for each passage were analysed to define the diploid number (2n) in a Zeiss
284 microscope Axio Imager Z2m.

285 DNA extraction of primary tissue and cell culture passages

286 Passage samples were extracted using the DNeasy Blood & Tissue Kit (Qiagen, Hilden,
287 Germany) following the manufacturer's protocol for cultured cells, while muscle tissue of the
288 same individual (collection ID ZFMK-TIS-50476) previously stored at LIB Biobank in 96%
289 ethanol (passage #0) was extracted using the standard protocol of the same kit. DNA
290 barcoding was performed to ensure species identity using primers for COI from Astrin and
291 Stüben (Astrin & Stüben, 2008) and sequences matched against BOLD (Barcode of Life Data
292 System) (Ratnasingham & Hebert, 2007).

293 Sequencing of primary tissue and passages

294 After DNA extraction, samples were sent for purification (Vahtstm DNA Clean Beads; Vazyme
295 Biotech, Nanjing, China), PCR-free library preparation (NEBNext Ultra II FS DNA PCR-free
296 Library Prep Kit for Illumina; NEB) and subsequent paired-end sequencing on a NovaSeq
297 6000 (Illumina, San Diego, USA) using the NovaSeq 6000 S4 Reagent Kit (Illumina) to
298 Biomarker Technologies (bmkgene; Beijing, China).

299 Read Mapping

300 The Illumina reads of all passages (passage 0, i.e. the primary tissue, three passage 5
301 replicate samples and four passage 10 replicate samples) were processed with fastp v. 0.20.0
302 (Chen et al., 2018) with parameters “--length_required 95, --qualified_quality_phred 20 --
303 adapter_fasta”, with a curated adapter list of the most common adapters used as input and
304 decontaminated with Kraken2 v2.1.3 with the Kraken database kraken2 PlusPFP database
305 downloaded in March 2023 in paired-read mode, with parameter “--paired --confidence 0.51 -
306 -use-names”. These reads were then mapped to the reference genome using BWA-MEM2

307 v2.2.1 (Li, 2013; Li & Durbin, 2009) with the *mem* command and options “-M -R”, where a read
308 group (RG) specific to each sample was used for “-R”. The resulting output was sorted using
309 SAMtools v1.19.2, and additional processing steps (SAMtools’ *fixmate*, *sort*, and *markdup*)
310 were performed to generate the final mapping files for each sample.

311 SNP Calling

312 SNP calling for each cell passage sample and the HiFi reads (“reference”) was performed
313 individually using GATK HaplotypeCaller v4.2.6.1 (Auwera & O’Connor, 2020; Poplin et al.,
314 2017) with the options “-ERC GVCF --min-base-quality-score 30 --pcr-indel-model NONE”.
315 Joint SNP calling was performed by first combining samples using GATK *GenomicsDBImport*
316 with the option “--batch-size 3”. The combined database was then used for joint SNP calling
317 with GATK’s *GenotypeGVCFs*.

318 Variant quality recalibration was conducted in three rounds. GATK’s *BaseRecalibrator* was
319 run with the option “--maximum-cycle-value 50000”, followed by GATK’s *ApplyBQSR* for each
320 sample before re-calling variants individually and collectively. From the final set of called
321 genotypes, SNPs were extracted using GATK’s *SelectVariants* with the option “-select-type
322 SNP” and filtered with GATK VariantFiltration using the filters: “QD < 2.0, FS > 60.0, MQ <
323 40.0, SOR > 3.0, MQRankSum < -12.5, ReadPosRankSum < -8.0, QUAL < 30.0”.

324 Variants were filtered for depth, minor allele frequency (MAF) and the fraction of missing
325 genotypes using BCFtools filter v1.21 (https://github.com/samtools/bcftools) with the options
326 “-e "INFO/DP<$MIN_DEPTH || INFO/DP>$MAX_DEPTH" ” and “-i "MAF>$MAF &&
327 F_MISSING<=$MISS".

328 Short-read variant analysis in passages

329 To assess the quality of the DNA contained in cell cultures and to understand its potential for
330 being used as an amplified genomic resource, these filtered SNPs were then analysed in R v
331 4.4.2. Passages #5 and #10 were compared to passage #0 and the HiFi reads at sites where

passages #5 and #10 differ from either of the reference passages. A Wilcoxon test from rstatix v 0.7.2 was performed to test whether the depth and GQ of these SNPs of each sample were significantly different from the average DP or GQ. The variant calls were re-coded so that: "0|0" = 0, "0|1" = 1, "1|0" = 1, "1|1" = 2, "0|2" = 3, "2|0" = 3, "1|2" = 4, "2|1" = 4, "2|2" = 5, "0|3" = 6, "3|0" = 6 and plotted with ggplot2.

Results

Read quality control and estimation of genome size and heterozygosity

After quality control, filtering, and decontamination the final set of HiFi reads used was composed of 5,078,732 million reads with a total length of ~58 Gbp and the HiC reads used were composed of 79.7 million reads with a total length of ~ 20Gbp.

Using a k-mer size of 21, genomescope was able to predict a genome size of 1,292,799,460 bp, a repeat length of 188,615,362 bp, a heterozygosity of 0.2% and a read error rate of 0.14%. Smudgeplot and GenomeScope also both verified the diploid status of the individual. (Supplementary Figure 1; Figure 2).

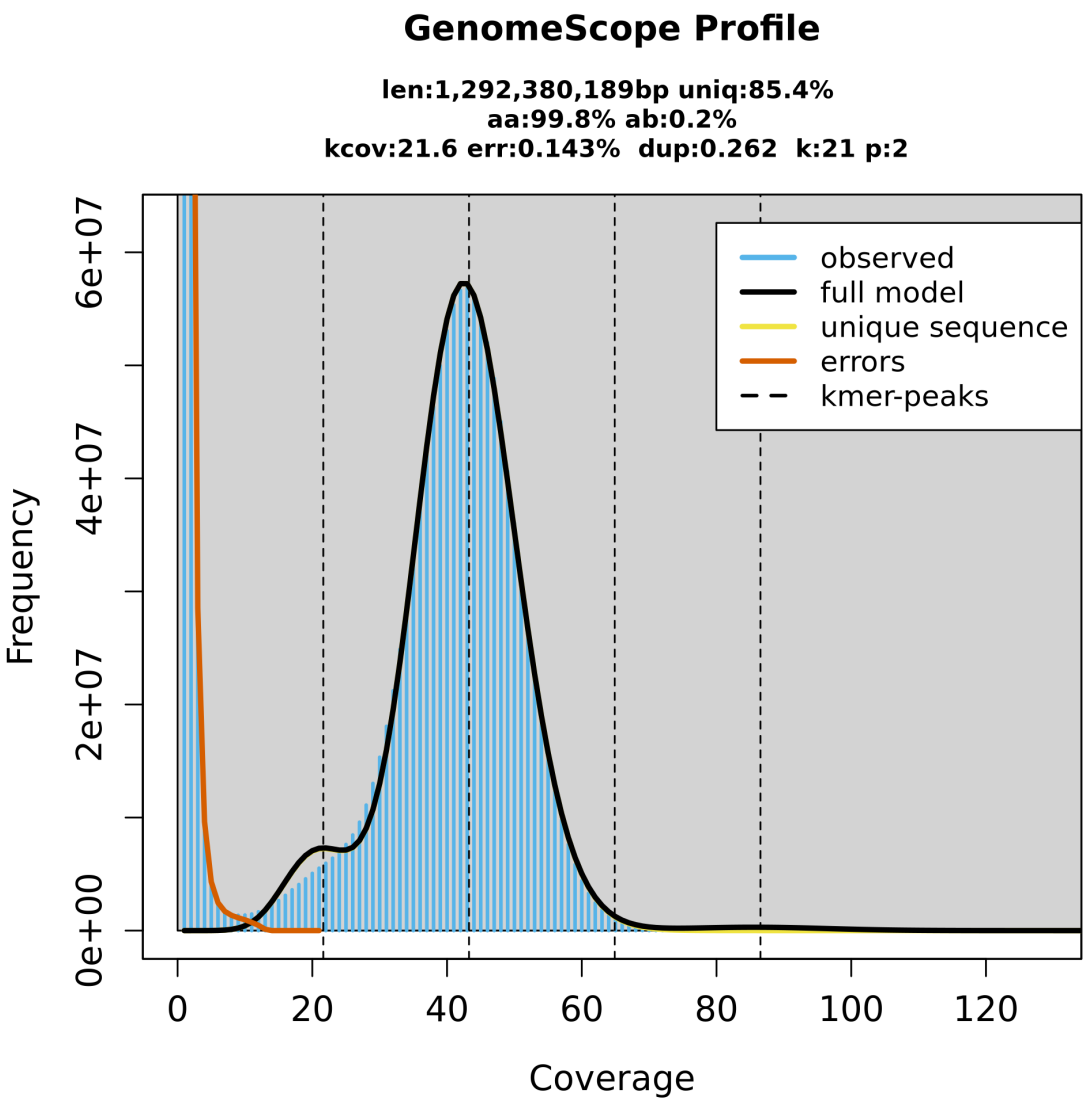

Figure 2: K-mer genome profile of *Strix uralensis* generated from PacBio HiFi reads with GenomeScope2.The y-axis shows the k-mer counts and the x-axis shows sequencing depth. The first peak corresponds to heterozygous k-mers and the second larger peak to homozygous k-mers with a coverage of ~42x.

Reference genome

The optimal assembly was created with hifiasm parameters “--n-weight 5 --n-perturb 50000 --f-perturb 0.5 -D 10 -N 150 -s 0.4” (Supplementary Table 1).

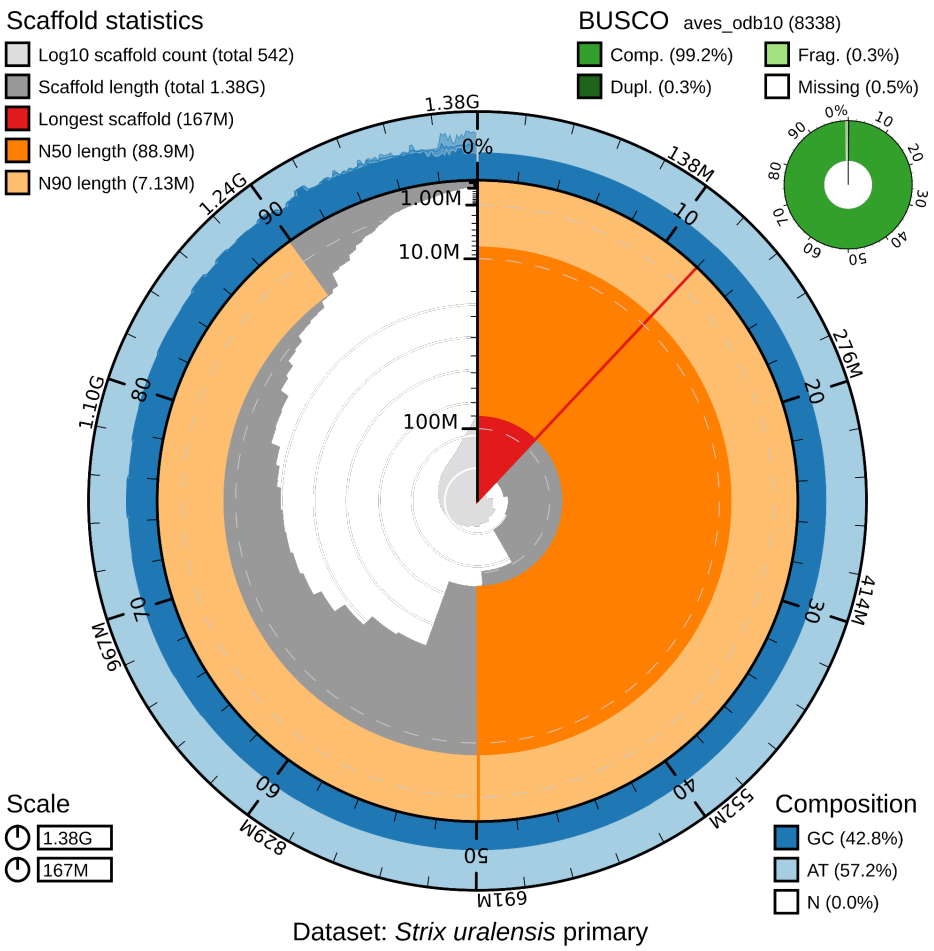

Figure 3: Snail plot summary of assembly statistics for *Strix uralensis* primary assembly. The main plot is divided into 1,000 size-ordered bins around the circumference with each bin representing 0.1% of the 1,381,000,783 bp assembly. The distribution of sequence lengths is shown in dark grey with the plot radius scaled to the longest sequence present in the assembly (166,530,430 bp, shown in red). Orange and pale-orange arcs show the N50 and N90 sequence lengths (88,922,949 and 7,132,230 bp), respectively. The pale grey spiral shows the cumulative sequence count on a log scale with white scale lines showing successive orders of magnitude. The blue and pale-blue area around the outside of the plot shows the distribution of GC, AT and N percentages in the same bins as the inner plot. A summary of complete, fragmented, duplicated and missing BUSCO genes in the aves_odb10 set is shown in the top right.

Genome Quality Metrics

We could place 93.6 % of assembled scaffolded genome sequence data into 41 chromosomes, which is consistent with the karyotype of the species (Figure 3). We also detected no contamination as all scaffolds aligned to sequences of other avian genomes (Figure 4). Our HiC contact map further supported the high contiguity of the primary assembly, by showing no remaining conflicts and little to no scaffolds with strong contacts to non-repeat regions (Figure 5).

The Merqury QV score, which is the proportion of the assembly sequence supported by HiFi reads, was estimated for both haplomes. We obtained a score of 64.175 (equivalent to an error probability of 3.8238e-07%) for the primary and 57.4252 (equivalent to an error probability of 1.80919e-06%) for the alternate assembly (Supplementary Table S2). We also find a completeness score of 98.36% for the primary and a combined 99.81% for the two haplomes, which is a fraction of the high-quality k-mers from the reads present in the assembly. This further supports the completeness and accuracy of the assembly (Supplementary Table S2).

Aligning the PacBio HiFi, and Illumina HiC reads to both haplomes revealed comparable coverage levels (primary: 41.78±12.18, 14.18±91.47-fold; alternate: 34.15±23.24, 12.10±107.37), mapping rates (primary: 99.85%, 99.92%; alternate: 80.52%, 86.6%) and mapping quality scores (primary: 36.93, 28.90; alternate: 28.11, 8.2). These results further indicate that the assembly is well-phased with a minimal amount of assembly bias and errors (Supplementary Table S3).

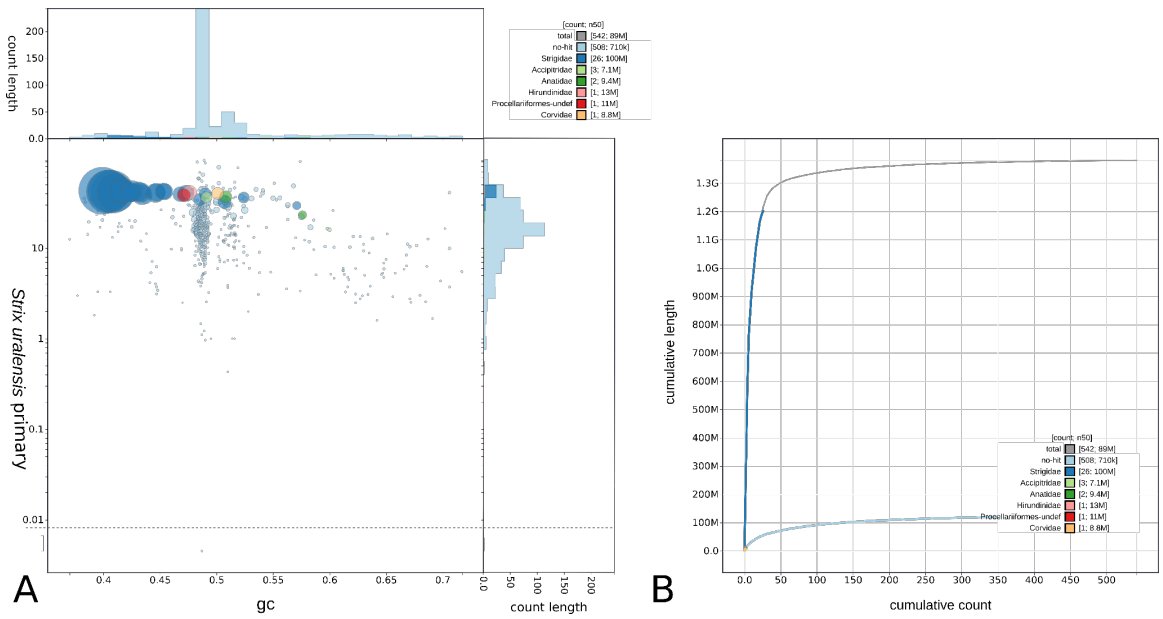

Figure 4: *Strix uralensis* assembly BlobToolKit GC-coverage and cumulative sequence plots. A) Blob plot of base coverage in *Strix uralensis* against GC proportion for sequences in *Strix uralensis* primary assembly. Sequences are coloured by phylum. Circles are sized in proportion to sequence length. Histograms show the distribution of sequence length sum along each axis. **B)** Cumulative sequence length for *Strix uralensis* primary assembly. The grey line shows cumulative length for all sequences. Coloured lines show cumulative lengths of sequences assigned to each phylum using the buscogenes taxrule.

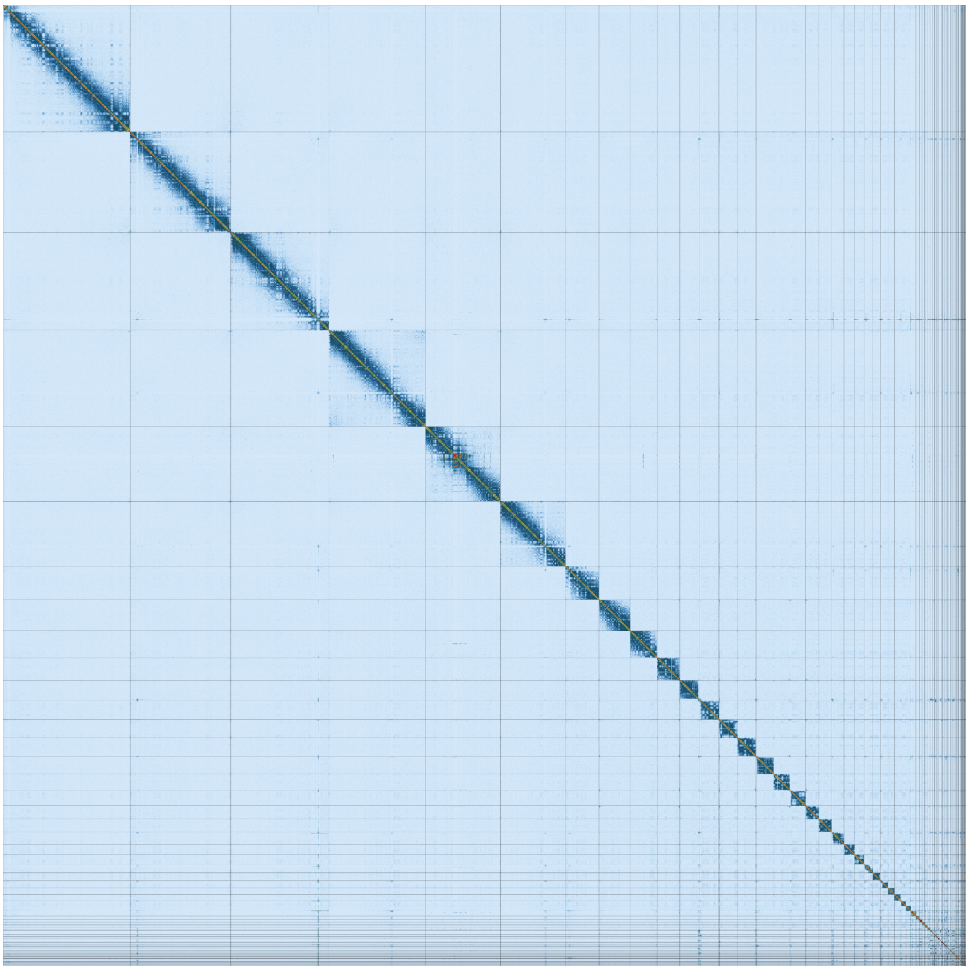

Figure 5: Hi-C contact map. Hi-C contact map of the *Strix uralensis* primary genome assembly, visualised with PretextView. Chromosomes are ordered by size from left to right and from top to bottom.

394 **Table 1**: Assembly statistics of the primary and alternate genome assembly of *Strix uralensis*.

Assembly statistics	**Primary**	**Alternate**
Assembly size [bp]	1,381,008,983	1,262,176,999
GC content [%]	42.77	42.81
Contigs	512	15,615
N50	90,173,155	17,018,198
L50	6	18
L90	28	8,171
Ns per 100 kbp	2.94	68.29
Merqury Error (%)	3.82794e-07	1.80919e-06
Merqury QV score	64.1703	57.4252
Complete BUSCOs [%]	99.94	70.82

Genome Repeat and Gene Annotation

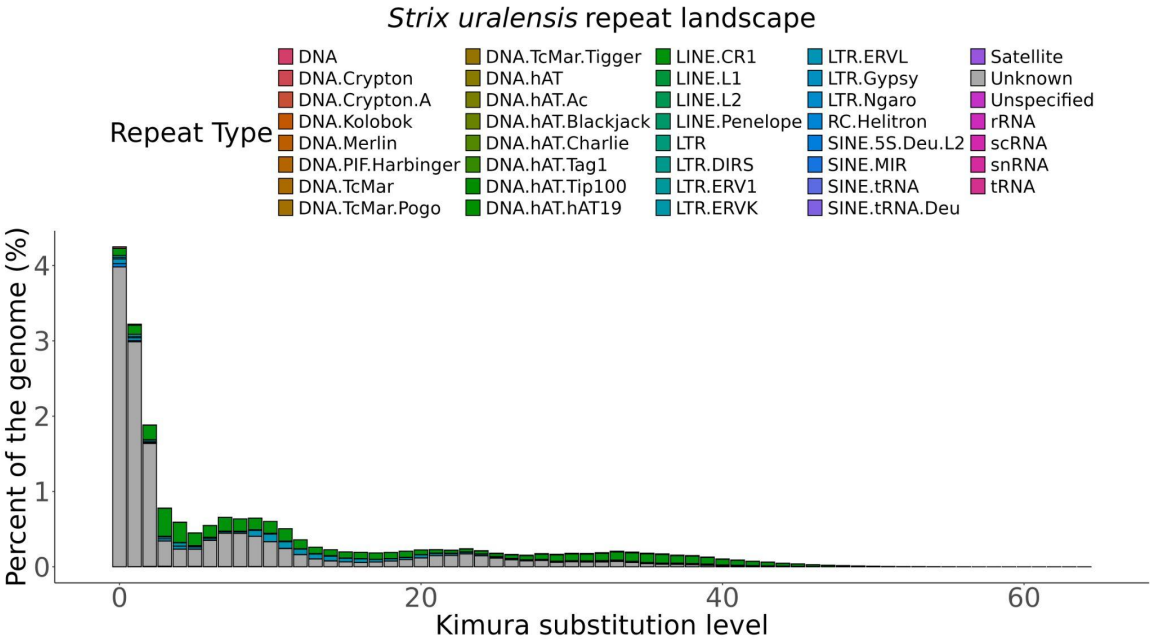

Figure 6: *Strix uralensis* repeat landscape. The genome assembly was masked using RepeatModeler and RepeatMasker. The plot shows the Kimura substitution of detected repeats.

Repeat landscapes depict the clustering of transposable elements (TEs) in relation to their Kimura substitution rates, which measure the divergence of TEs from their respective consensus sequences. Lower Kimura substitution rates indicate recent transposition events, while higher rates suggest older events. From the landscape of the primary assembly, a strong signal for very recent repeat expansion as well as a well-maintained large amount of older ones are visible. This might support a repeat expansion in the Ural Owl or the genus *Strix*. That the majority of the repeats under these two expansion peaks are not annotated would further suggest that they are either a new or unique feature of *Strix* and a reference or consensus might not yet exist in the present databases, like the DFam used here. The repeat landscape of the alternate assembly can be found in Supplementary Figure 2.

Gene annotation

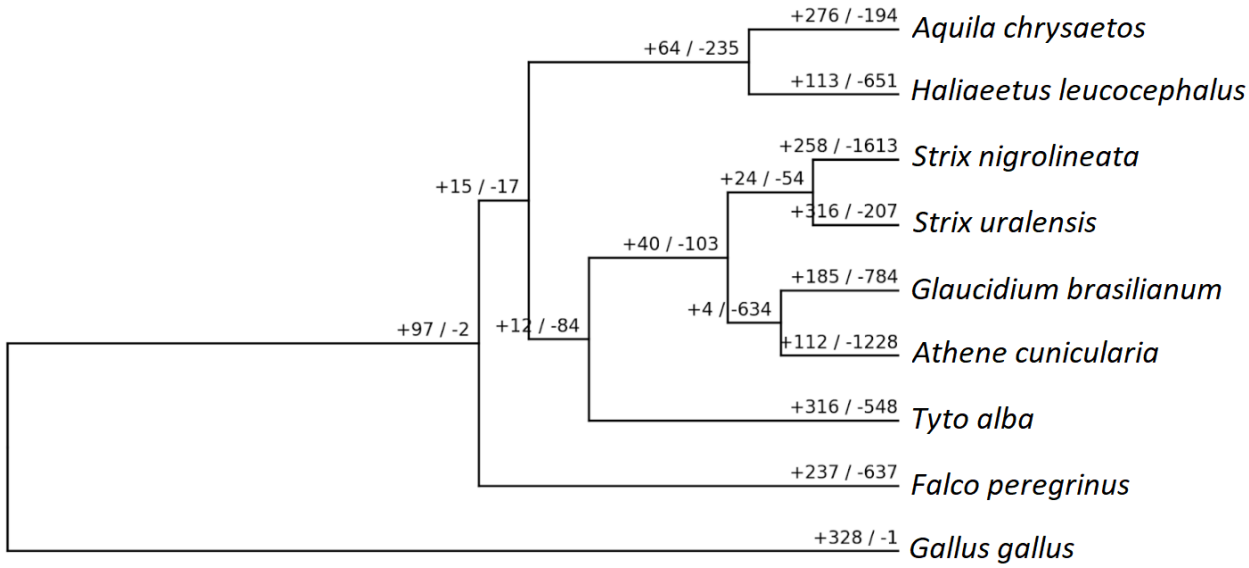

Figure 7: Ultrametric phylogenetic tree of selected Neoaves species and *Strix uralensis*. Numbers indicate gene family expansions (+) and contractions (-).

For the primary assembly, we were able to annotate a total of 17,977 protein-coding genes which cover ~33.6% of the total size of the assembly (Supplementary Table S 4). We detected 182,313 exons and 164,373 introns. When compared to the Swiss-Prot and Trembl databases we were able to match 17,590 and 16,483 genes respectively (Supplementary Table S 5).

To shed some light on the genome annotation content, we compared the Ural Owl genome to other high-quality genomes of the Aves lineage, including several owl species. Gene expansion (gain) and contraction (loss) among our selected species found 316 gene family gains in the Ural Owl and 207 gene losses, 168 of which were, presumably, completely lost and, thus, have no representative in the Ural Owl genome assembly (Figure 7). Additionally, we found 81 gene families unique to the Ural Owl that do not have orthologs in the other species. We further found that genomes of lower quality, such as those of the Ferruginous pygmy owl, *Glaucidium brasilianum,* and the Black-and-white Owl, *Strix nigrolineata*, had more gene losses, which are hence probably not biologically true. A GO Term analysis of the genes unique to the Ural Owl revealed many interesting gene

428 families that due to the low quality of the Black-and-white Owl genome might also be
429 interpreted as partially representing the *Strix* genus (Figure 8). Among these categories we
430 note several GO terms relevant to the unique traits of the owls, namely their adaptation to dim-
431 light conditions and their unique hunting strategy, which is mostly sedentary and predatory. In
432 the "animal organ development" parent GO Term we can find GO Terms for "eye
433 development", "sensory organ development", "neurogenesis" and "heart development", all of
434 which point to adaptations of *Strix*, either to their environment or lifestyle.

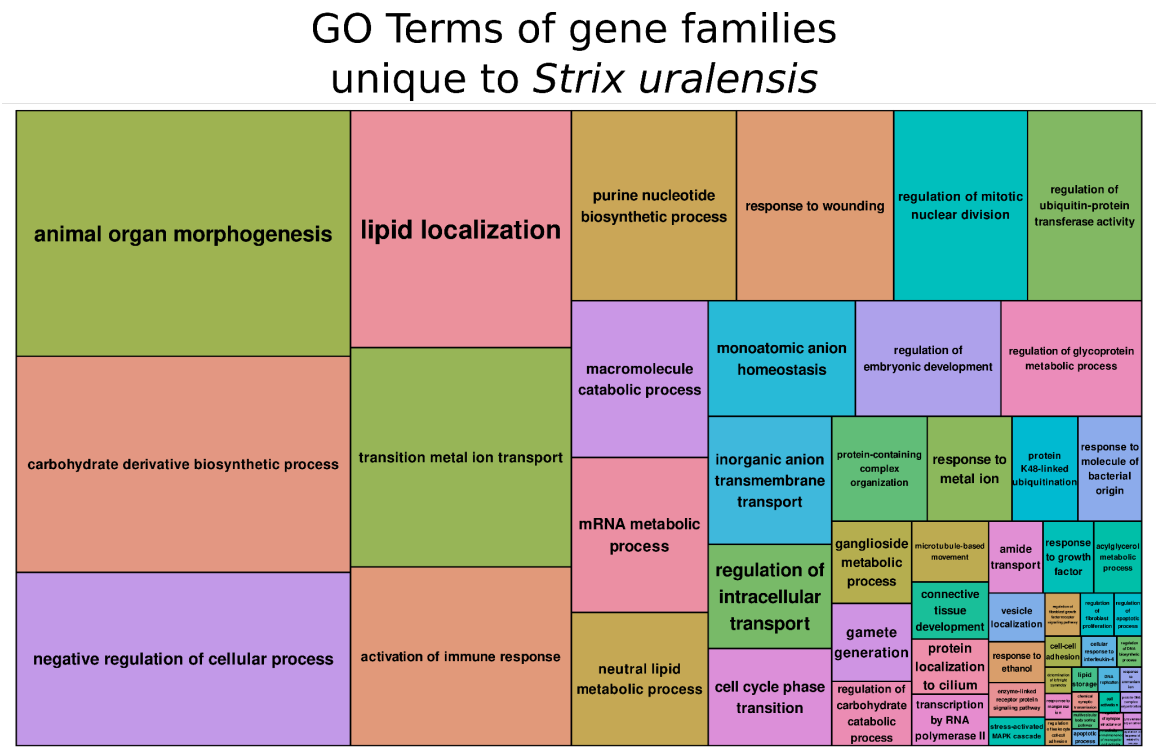

435 **Figure 8: Treemap plot of most frequent GO Term categories of gene families unique to**
436 ***Strix uralensis.*** Colour of sections is unique to each category and the size scales positively
437 with the GO Term frequency.

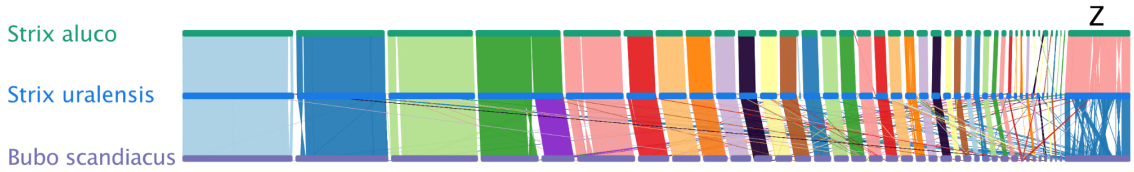

Figure 9: Chromosome scale synteny analysis. Synteny of chromosomes of *S. aluco* (top) and *Bubo scandiacus* (bottom) compared to the newly sequenced *S. uralensis* (middle). Syntenic regions amongst the species are indicated with a unique colour. Plot made with NGenomeSynt. Only scaffolds that mapped to the *S. uralensis* chromosomes were included. Assignment of sex chromosomes is based on the *S. aluco* genome annotation.

Chromosome Scale Syntenies

Synteny with the chromosome-level assemblies of *Strix aluco* and *Bubo scandiacus* confirmed the male sex of the sequenced Ural Owl genome by identifying its Z chromosome. It is the fifth largest chromosome in the Ural Owl assembly (chromosome 5). The synteny between the two *Strix* genomes shows no major syntenic differences. This is also mostly true in the comparison to the Snowy Owl with the exception of the Z chromosome, which shows some internal rearrangements compared to the two *Strix* species. If this is caused by assembly quality and accuracy remains to be investigated. Additionally, we detect a possible chromosome fusion of chromosomes 5 and 6 of the Snowy Owl into chromosome 4 of the two *Strix* assemblies. This is supported by previous cytogenetic analyses (Yamada et al., 2004).

Demographic history

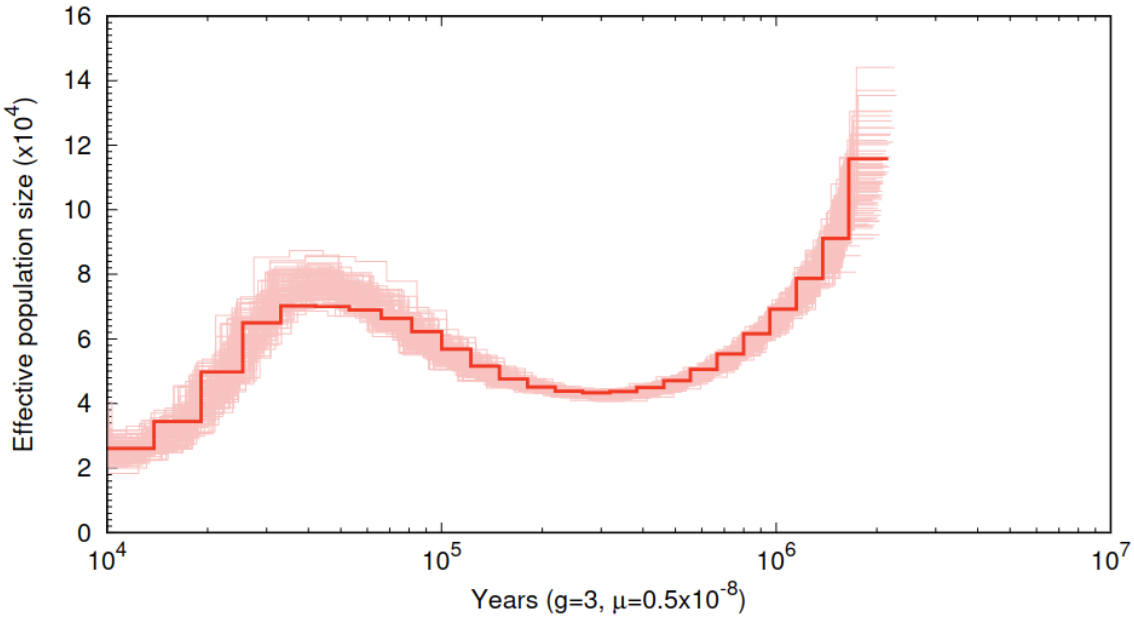

Figure 10. Inferred demographic history of *Strix uralensis* from PSMC analysis based on the primary assembly. The x-axis shows years before present (ya) on a logarithmic scale and the y-axis shows the estimated effective population size. Bootstrap results are shown as transparent lines.

The demographic history of the Ural Owl derived from our genome assembly appears to have a complex relationship to glacial and interglacial periods. The effective population was predicted to have decreased until around the Holstein interglacial period (3.74 × 10^5 – 4.24 × 10^5 ya) where its population size stabilized but remained low during the Saalian glacial period (4-1.3 × 10^5 ya) and began to increase as the Eemian interglacial period (1.3-1.15 × 10^5 ya) began to emerge. It continued to increase and reached a plateau during the last glacial period (Weichselian glaciation, 1.15-0.117 × 10^5 ya). This pattern would suggest at least some level of tolerance to lower temperature climates that is, however, not absolute since the Ural Owl population began to decrease before the end of the last glacial period, at around 0.3 ×10^5 ya. It is also possible that the effects of the glacial period were confounded by the increased activity of *Homo sapiens* in Europe during this period.

Variation analysis over progressive cell passages

Karyotype confirms chromosome numbers and reveals no large variants caused by passaging

Chromosomal analyses detected 2n=82 in both passages #5 and #10, corroborating the diploid chromosome number described for the Ural Owl (subspecies *S. uralensis uralensis* and *S. u. japonica*) previously (Takagi & Sasaki, 1974) and no large-scale chromosomal rearrangements were observed between both passages (Figure 11).

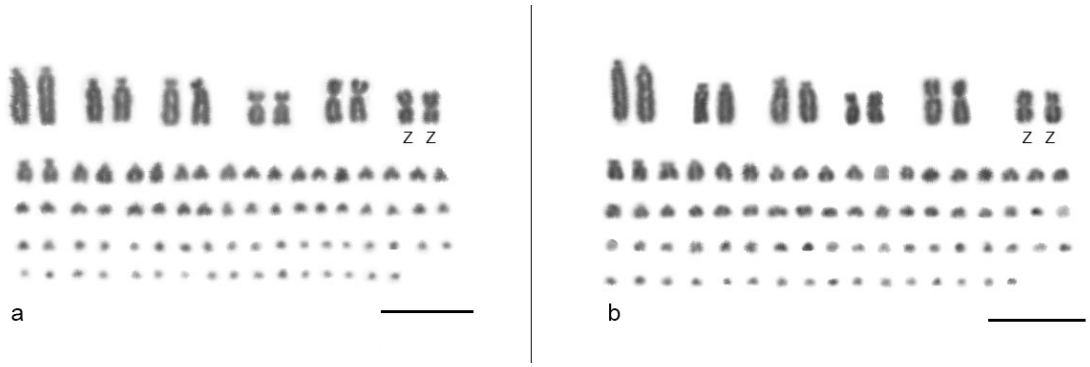

Figure 11: Karyotype analysis. Karyotype of *Strix uralensis* male with 2n=82 after passage 5 (a) and passage 10 (b). Bar=10µm.

Short-read variants

After quality filtering, we identified 885,159 variant sites (in the following referred to as SNPs) (Figure 12). Out of these, the vast majority (i.e., 670,463 SNPs) were fixed variant sites across all samples and hence mostly represented heterozygous sites of the individual which are represented with just one of the two alleles in the reference genome or sites that had a wrong allele in the reference assembly.

The remaining 214,696 SNPs varied across samples, indicative of potential mutations, and were analysed in the following.

A comparison of all SNPs across all samples revealed that variant amount and type differed. The biggest differences resulted from SNPs called from the HiFi data as well as the passages

5.1 and 10.1 which appear to have more SNPs than the other passages. The majority of these are heterozygous first-alternate sites (Figure 12; Table 2) and we suspect for many of those that they are false heterozygous calls rather than true mutations. To investigate this pattern further, we inspected genotype quality and depth focusing on sites with a genotype in a sample not found in any other sample (referred to as private sites) compared to the same metrics at all other sites of that individual (i.e., common variants and conserved heterozygous sites). This analysis revealed that all passages had similar median depth per variant site (DP ~ 26.78±6.55) and genotype quality (GQ ~99), suggesting rather consistent data quality across samples (Table 2). It further showed that median depth and quality of private SNPs consistently had a significantly lower depth and quality than the average non-private site, suggesting that these alleles are to some extent wrongly called (Figure 13). To account for patterns potentially driven by sequencing technology, we also assessed in each replicate at how many positions it differed compared to passage 0. This revealed the same pattern of an increase of SNPs in samples passage #5.1 and #10.1

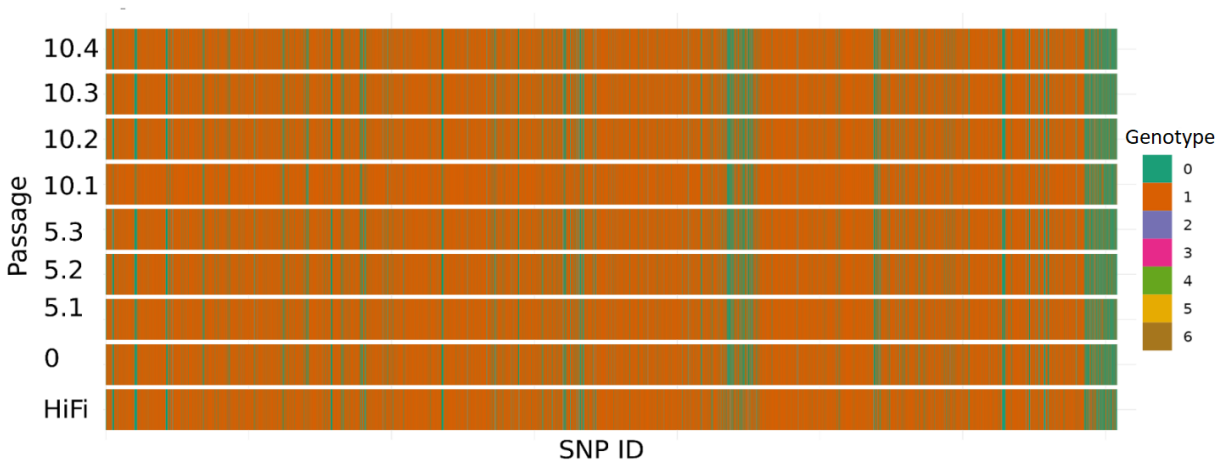

Figure 12: Variant calls of each passage. SNPs are ordered by genome position as derived from the variant filed, colour indicates allele as illustrated in the inset and referring to I "0|0" = 0, "0|1" = 1, "1|0" = 1, "1|1" = 2, "0|2" = 3, "2|0" = 3, "1|2" = 4, "2|1" = 4, "2|2" = 5, "0|3" = 6, "3|0" = 6.

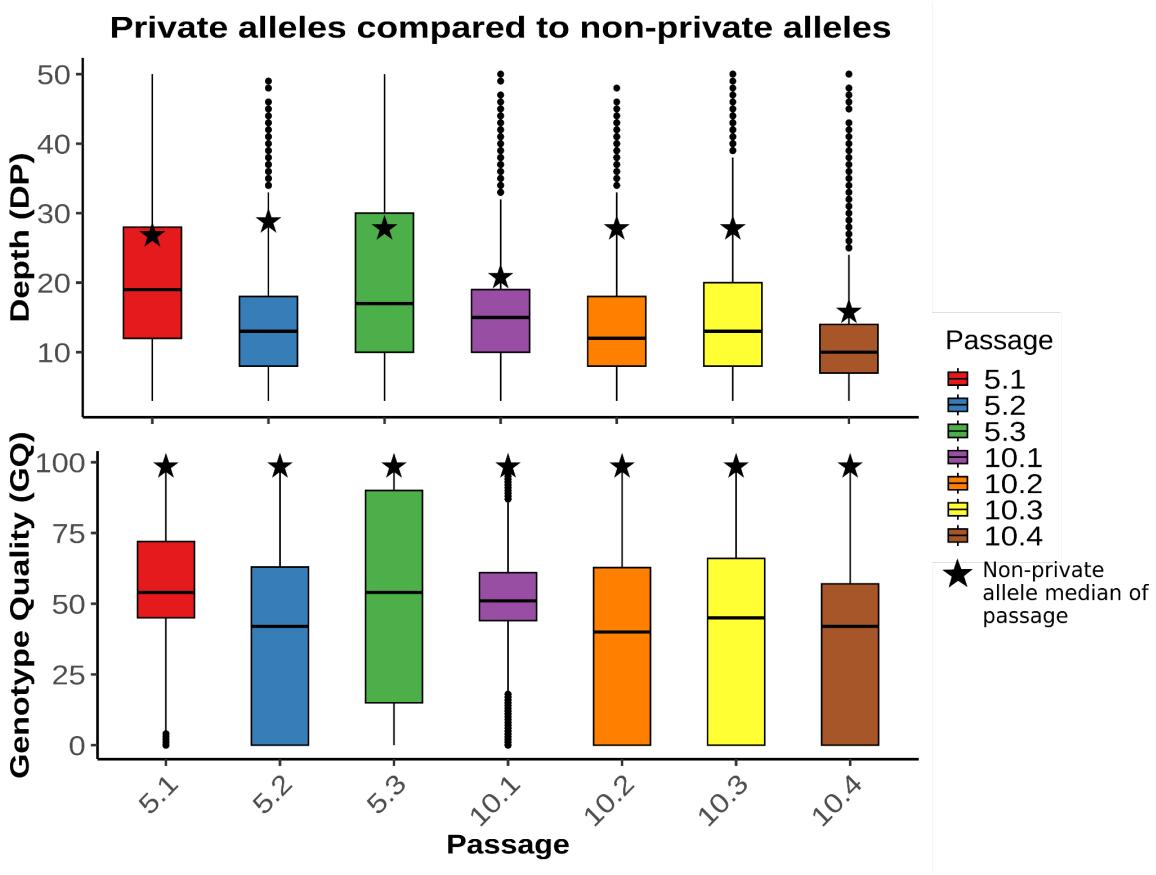

508 **Figure 13: Quality assessment of private sites.** Median depth (top) and median genotype
509 quality (bottom) of private SNPs in each section compared to non-private SNPs (star).

510 **Table 2**: SNP statistics over progressive cell culture passages.

Sample	Median depth of variant sites	Median GQ of variant sites	SNPs other than shared heterozygous sites/private to individual	SNPs other than shared heterozygous sites as a percentage of the total genome size [%]	SNPs that are 0/1	SNPs that are not 0/1 nor 1/1	SNPs other than fixed heterozygous sites [%]	SNPs different from passage #0	SNPs different from passage #0 [%]
HiFi Reads	39	99	78,983/35,645	0.0057	77,682	1,265	0.14	-	-
Passage #0	27	99	57,929/8,212	0.0042	56,232	816	0.922	-	-
Passage #5.1	27	99	78,193/23,889	0.0057	76,709	716	0.809	58,620	6.62
Passage #5.2	29	99	55,225/3,280	0.0040	54,037	615	0.695	38,765	4.38
Passage #5.3	28	99	57,664/5,581	0.0042	56,267	781	0.882	41,301	4.67
Passage #10.1	20	99	103,086/63,058	0.0075	101,450	25	0.028	96,768	10.93
Passage #10.2	28	99	54,404/3,410	0.0039	53,373	420	0.475	38,921	4.40
Passage #10.3	28	99	55,976/3,758	0.0041	54,679	642	0.725	39,843	4.50
Passage #10.4	15	99	54,215/15,521	0.0039	52,153	750	0.847	50,033	5.65

511

Discussion

Reference genomes are accumulating across the tree of life and concerning this trend, birds have seen special attention fuelled by initiatives such as B10K (https://b10k.com/). Still, many of these genomes remain incomplete in terms of chromosomal-scale assembly type as well as gene annotation comprehensiveness. Genome assembly quality can impact phylogenomic inferences, analyses of gene prediction, gene family expansion and contraction, and most importantly structural evolution. In an effort to allow such analysis for the vastly understudied bird order Strigiformes, we here present a reference genome for the Ural Owl, that is of very high quality and among the best bird genome assemblies currently, reflected by assessments of sequence and gene completeness. Most of the genome could be placed in chromosomal scale scaffolds and is in line with the species karyotype, that e also confirm. We further identified the supposedly *Strix*-specific chromosomal fusion which distinguishes it from the genus *Bubo* (Rebholz et al., 1993). An initial analysis of the Ural Owl genome content indicates an important increase in repeat content. Birds on average have rather compact genomes compared to other vertebrate lineages (average ~1.1Gb (Feng et al., 2020)), mostly owing to a low content of repetitive elements (10-15%). Until now, owls were seemingly no exception to this with an average genome size of 1.2Gb and a repeat content of ~8,6% (Feng et al., 2020). Still, cytogenetic studies already suggested differently and hint at owls being rather an exception in the avian lineage with large scale variations in karyotypes. For example, the barn owls have no distinct macro- and micro-chromosomes whereas the true owls do, suggesting a role for chromosome fusion and fission in owls. Interestingly, the recently published genome (1.6Gb) of the Snowy Owl further extends this suspicion by demonstrating that it has one of the highest reported repeat contents for birds (28.34%), mainly composed of centromeric satellite DNA (Baalsrud et al., 2024). Our assembly's total repeat content, at around 21% (11% of which is unidentified), follows this pattern. In the Snowy Owl, the repeats are suspected to have driven the evolution of novel centromeres. Accordingly, cytogenetic analyses already identified large centromeric satellite blocks shared among and unique to true owls (Yamada

539 et al., 2004). Other bird lineages with increased repeat content are woodpeckers and the
540 Common Scimitarbill (*Rhinopomastus cyanomelas*) (Feng et al., 2020). The cause and
541 consequences of the repeat extensions in the genera *Strix* and *Bubo* remain unclear at this
542 point, which is also true for the woodpecker (Forest et al., 2024).

543 Our assembly seems to be particularly well-suited for an analysis of gene content since our
544 gene completeness analysis supports high completeness of gene annotation. Due to vastly
545 varying assembly qualities, we cannot guarantee the correctness of our gene family expansion
546 analysis. Still, this preliminary analysis suggests that in the future we will be able to connect
547 changes in gene content to adaptations of owls. This is supported by gene gains in the GO-
548 term derived function of e.g. “eye development”, “sensory organ development” and
549 “neurogenesis”, which could be linked to adaptations required for a nocturnal, predatory
550 lifestyle (Borges et al., 2015).

551 The Ural Owl is protected under the CITES convention Annex II and the Bern Convention on
552 the Conservation of European Wildlife and Natural Habitats. While globally not yet under
553 concern, the species went extinct in Germany and other parts of Europe due to habitat
554 destruction but also direct persecution. It has subsequently been reintroduced, however due
555 to low availability of breeding couples, individuals of various origins were used for these
556 actions (Scherzinger, 2006). Breeding efforts for the species are currently undertaken by
557 several zoos and raptor centres and the European conservation breeding program for this
558 species is coordinated by the Parc animalier de Sainte-Croix in France. An analysis of marker
559 genes neither supported morphological subspecies nor did it reveal a phylogeographic
560 population structure for the Ural Owl. Yet, it revealed genetic clusters that could be informative
561 for supportive breeding programs (Hausknecht et al., 2014). The here generated reference
562 genome will facilitate future genomic studies int his direction of *S. uralensis*.

563 Simultaneously, the genome already shed light on the demographic history of the species
564 further supporting important population contractions. Interestingly however, our analyses also
565 suggested an increase in population size during the last glacial period before decline brought

566 it further down. This questions climate changes as the sole effect of population changes prior
567 to intensified habitat destruction and hunting in the younger past, which drove the species
568 extinct in parts of Europe.

569 Also, in the light of species preservation, protection and restoration, *ex situ* efforts are gaining
570 more attention. Cell culturing is a valuable and widely used technique, spanning applications
571 from basic science to biotechnology research (Freshney, 2010). Cells carry copies of genetic
572 information, offering crucial molecular insights into the respective species. However, to date,
573 there is no consensus regarding the number of passages considered "safe" before cells
574 experience metabolic changes, DNA damage, and chromosomal instability. What is deemed
575 "high passage" for one cell culture may not lead to significant passage effects in another
576 (Hughes et al., 2007). Thus, the effects of prolonged culture are complex and vary depending
577 on the individual cell culture, tissue, and species.

578 The first criterion for identifying healthy and stable cells is observing cell morphology.
579 Chromosome content serves as another critical benchmark, as normal cells maintain a stable
580 chromosome number. Few studies using non-model species such as felines (Song et al.,
581 2007) and fishes (Alvarez et al., 1991) showed no heteroploidy on karyotypes obtained by cell
582 cultures. However, to the best of our knowledge, this is the first study that addresses genomic
583 and chromosome changes in wild birds and compares the effect of different cell passages on
584 genome integrity.

585 Cryopreservation of cells has increasingly been considered a strategy for conservation as new
586 technologies using genetic material from somatic cells (e.g. somatic cell nuclear transfer or
587 induced pluripotent stem cells) are evolving (Bolton et al., 2022; Mooney et al., 2023). One of
588 the prerequisites for nuclear donor cells and *ex situ* conservation is the stability of
589 chromosomes (Song et al., 2007).

590 Herein, comparison between karyotypes of passage 5 and passage 10 showed no differences,
591 suggesting that no large structural rearrangement occurred during the progressive number of
592 passages and that it is safe to establish the diploid number of (this) bird species until at least
593 the 10th passage. Studies that investigate cell line passage and age effects are still scarce in
594 non-model organisms and are crucial since altered metabolism and genomic instability no
595 longer represent reliable models of their original source of material.

596 Genetic instability is well-documented in cells that have undergone more than 20 passages,
597 particularly in transformed continuous cell lines (e.g. (Odoemelam et al., 2009)) and tumour
598 cell lines (Z. He et al., 2023; Wenger et al., 2005). However, for primary cell cultures, a
599 straightforward method to determine the safest passage number before cells develop
600 mutations or genetic instability remains lacking. In this study, we opted to cultivate the cells
601 up to passage 10. This decision was based on two factors: first, the uncertainty surrounding
602 the exact passage limit at which primary cells may enter senescence (as non-continuous cell
603 line has limited in vitro life time); and second, technical challenges observed during later
604 passages as cells began to exhibit signs of morphological decline, including the presence of
605 granules and debris, difficulty detaching, and a reduced growth rate, all of which would
606 complicate further subculturing beyond passage 10.

607 This seems to suggest rather safe cell culturing for this species until passage 10. To some
608 extent, this is supported by our SNP analysis of several passage replicates which indicated
609 no general pattern for increased genomic changes between passages 5 and 10. However, we
610 detected outlier samples with respect to SNP numbers among replicates of both passage
611 numbers. At this point, we lack any point of reference expectation as to how many (potential)
612 mutations are to be expected in a cell culture system as the one we applied. Compared to
613 overall levels of variant sites, the number of SNPs in the individual samples which could be
614 mutations is lower and represented between 0.0039-0.0075 % of the genome assembly
615 length. The effects of these variants remain to be determined as well as the reason for between
616 replicate differences. We further suspect that several mutations are variant-calling artefacts,

617 supported by lower SNP calling quality, which asks for an exploration of mutation identification

618 and more importantly validation for the type of cell culture we have set up here.

Data Availability Statement

Sequencing reads, assembly and BioSample information are available at NCBI Project number PRJNA1212906. Supplementary material is available at https://zenodo.org/records/14711423.

Acknowledgments

This work was supported by the Leibniz Gemeinschaft Leibniz Association Network grant CollOmic K419/2021 to AB and LIB innovation fund to AB and JA.

Conflict of Interest

The authors declare no conflict of interest.

Funder Information

AB and IC are supported by the Leibniz Association Network grant CollOmic K419/2021. IC, AM, CBDN, JA and AB are supported by the Leibniz Association.

Authors' contributions

AB and JA designed the project with input from IC, AM and CBDN. AB, TT, AM, JA, and IC led the writing and devising of the manuscript. DF provided the sample. NS and BH performed reference genome sequencing. IC performed genome assembly and annotation, gene family evolution, gene ontology term analysis and demographic history analyses. IC and AM performed SNP calling analysis. AM and CBDN performed library preparation, cell culture and karyotyping. LvM helped with cell culturing. All authors contributed to the manuscript revision.

References

Able, K. P. (2000). Handbook of the Birds of the World, Volume 5, Barn-owls to Hummingbirds. *The Auk*, *117*(2), 532–534. https://doi.org/10.1093/auk/117.2.532

Afgan, E., Baker, D., Batut, B., van den Beek, M., Bouvier, D., Čech, M., Chilton, J., Clements, D., Coraor, N., Grüning, B. A., Guerler, A., Hillman-Jackson, J., Hiltemann, S., Jalili, V., Rasche, H., Soranzo, N., Goecks, J., Taylor, J., Nekrutenko, A., & Blankenberg, D. (2018). The Galaxy platform for accessible, reproducible and collaborative biomedical analyses: 2018 update. *Nucleic Acids Research*, *46*(W1), W537–W544. https://doi.org/10.1093/nar/gky379

Allio, R., Schomaker-Bastos, A., Romiguier, J., Prosdocimi, F., Nabholz, B., & Delsuc, F. (2020). MitoFinder: Efficient automated large-scale extraction of mitogenomic data in target enrichment phylogenomics. *Molecular Ecology Resources*, *20*(4), 892–905. https://doi.org/10.1111/1755-0998.13160

Altschul, S. F., Gish, W., Miller, W., Myers, E. W., & Lipman, D. J. (1990). Basic local alignment search tool. *Journal of Molecular Biology*, *215*(3), 403–410. https://doi.org/10.1016/S0022-2836(05)80360-2

Alvarez, M. C., Otis, J., Amores, A., & Guise, K. (1991). Short-term cell culture technique for obtaining chromosomes in marine and freshwater fish. *Journal of Fish Biology*, *39*(6), 817–824. https://doi.org/10.1111/j.1095-8649.1991.tb04411.x

Astrin, J. J., & Stüben, P. E. (2008). Phylogeny in cryptic weevils: Molecules, morphology and new genera of western Palaearctic Cryptorhynchinae (Coleoptera:Curculionidae). *Invertebrate Systematics*, *22*(5), 503. https://doi.org/10.1071/IS07057

Auwera, G. V. der, & O'Connor, B. D. (2020). *Genomics in the cloud: Using Docker, GATK, and WDL in Terra* (First edition). O'Reilly.

Axelsson, E., Webster, M. T., Smith, N. G. C., Burt, D. W., & Ellegren, H. (2005). Comparison of the chicken and turkey genomes reveals a higher rate of nucleotide divergence on

663 microchromosomes than macrochromosomes. *Genome Research*, *15*(1), 120–125.
664 https://doi.org/10.1101/gr.3021305

665 Baalsrud, H. T., Garmann-Aarhus, B., Enevoldsen, E. L. G., Krabberød, A. K., Fischer, D.,
666 Tooming-Klunderud, A., Skage, M., Árnyasi, M., Sandve, S. R., Jakobsen, K. S., Nielsen, R.,
667 Boessenkool, S., & Tørresen, O. K. (2024). Evolutionary new centromeres in the snowy owl
668 genome putatively seeded from a transposable element.
669 https://doi.org/10.1101/2024.07.05.602039

670 Benson, G. (1999). Tandem repeats finder: A program to analyze DNA sequences. *Nucleic*
671 *Acids Research*, *27*(2), 573–580. https://doi.org/10.1093/nar/27.2.573

672 Béziers, P., & Roulin, A. (2021). Sexual maturity varies with melanic plumage traits in the barn
673 owl. *Journal of Avian Biology*, *52*(7), jav.02715. https://doi.org/10.1111/jav.02715

674 Bolton, R. L., Mooney, A., Pettit, M. T., Bolton, A. E., Morgan, L., Drake, G. J., Appeltant, R.,
675 Walker, S. L., Gillis, J. D., & Hvilsom, C. (2022). Resurrecting biodiversity: Advanced assisted
676 reproductive technologies and biobanking. *Reproduction and Fertility*, *3*(3), R121–R146.
677 https://doi.org/10.1530/RAF-22-0005

678 Borges, R., Khan, I., Johnson, W. E., Gilbert, M. T. P., Zhang, G., Jarvis, E. D., O'Brien, S. J.,
679 & Antunes, A. (2015). Gene loss, adaptive evolution and the co-evolution of plumage
680 coloration genes with opsins in birds. *BMC Genomics*, *16*(1), 751.
681 https://doi.org/10.1186/s12864-015-1924-3

682 Brommer, J. E., Pietiäinen, H., & Kolunen, H. (2002). Reproduction and survival in a variable
683 wnvironment: Ural Owls (*Strix uralensis*) and the three-year vole vycle. *The Auk*, *119*(2), 544–
684 550. https://doi.org/10.1093/auk/119.2.544

685 Brůna, T., Li, H., Guhlin, J., Honsel, D., Herbold, S., Stanke, M., Nenasheva, N., Ebel, M.,
686 Gabriel, L., & Hoff, K. J. (2023). Galba: Genome annotation with miniprot and AUGUSTUS.
687 *BMC Bioinformatics*, *24*(1), 327. https://doi.org/10.1186/s12859-023-05449-z

688 Burt, D. W. (2002). Origin and evolution of avian microchromosomes. *Cytogenetic and*

Genome Research, *96*(1–4), 97–112. https://doi.org/10.1159/000063018

Cantalapiedra, C. P., Hernández-Plaza, A., Letunic, I., Bork, P., & Huerta-Cepas, J. (2021). eggNOG-mapper v2: Functional annotation, orthology assignments, and domain prediction at the metagenomic scale. *Molecular Biology and Evolution*, *38*(12), 5825–5829. https://doi.org/10.1093/molbev/msab293

Challis, R., Richards, E., Rajan, J., Cochrane, G., & Blaxter, M. (2020). BlobToolKit – Interactive quality assessment of genome assemblies. *G3 Genes|Genomes|Genetics*, *10*(4), 1361–1374. https://doi.org/10.1534/g3.119.400908

Chen, S., Zhou, Y., Chen, Y., & Gu, J. (2018). fastp: An ultra-fast all-in-one FASTQ preprocessor. *Bioinformatics*. https://doi.org/10.1101/274100

Cheng, H., Concepcion, G. T., Feng, X., Zhang, H., & Li, H. (2021). Haplotype-resolved de novo assembly using phased assembly graphs with hifiasm. *Nature Methods*, *18*(2), 170–175. https://doi.org/10.1038/s41592-020-01056-5

Cramp, S. (1989). *Handbook of the birds of Europe, the Middle East, and north Africa: The birds of the western Paleartic*. Oxford university press.

Danecek, P., Bonfield, J. K., Liddle, J., Marshall, J., Ohan, V., Pollard, M. O., Whitwham, A., Keane, T., McCarthy, S. A., Davies, R. M., & Li, H. (2021). Twelve years of SAMtools and BCFtools. *GigaScience*, *10*(2), giab008. https://doi.org/10.1093/gigascience/giab008

Degrandi, T. M., Barcellos, S. A., Costa, A. L., Garnero, A. D. V., Hass, I., & Gunski, R. J. (2020). Introducing the bird chromosome database: An overview of cytogenetic studies in birds. *Cytogenetic and Genome Research*, *160*(4), 199–205. https://doi.org/10.1159/000507768

Ellegren, H. (2010). Evolutionary stasis: The stable chromosomes of birds. *Trends in Ecology & Evolution*, *25*(5), 283–291. https://doi.org/10.1016/j.tree.2009.12.004

Emms, D. M., & Kelly, S. (2019). OrthoFinder: Phylogenetic orthology inference for

comparative genomics. *Genome Biology*, *20*(1), 238. https://doi.org/10.1186/s13059-019-1832-y

Feng, S., Stiller, J., Deng, Y., Armstrong, J., Fang, Q., Reeve, A. H., Xie, D., Chen, G., Guo, C., Faircloth, B. C., Petersen, B., Wang, Z., Zhou, Q., Diekhans, M., Chen, W., Andreu-Sánchez, S., Margaryan, A., Howard, J. T., Parent, C., … Zhang, G. (2020). Dense sampling of bird diversity increases power of comparative genomics. *Nature*, *587*(7833), 252–257. https://doi.org/10.1038/s41586-020-2873-9

Flynn, J. M., Hubley, R., Goubert, C., Rosen, J., Clark, A. G., Feschotte, C., & Smit, A. F. (2020). RepeatModeler2 for automated genomic discovery of transposable element families. *Proceedings of the National Academy of Sciences*, *117*(17), 9451–9457. https://doi.org/10.1073/pnas.1921046117

Forest, T., Achaz, G., Marbouty, M., Bignaud, A., Thierry, A., Koszul, R., Milhes, M., Lledo, J., Pons, J.-M., & Fuchs, J. (2024). Chromosome-level genome assembly of the European green woodpecker *Picus viridis*. *G3: Genes, Genomes, Genetics*, *14*(5), jkae042. https://doi.org/10.1093/g3journal/jkae042

Freshney, R. I. (2010). *Culture of animal cells: A manual of basic technique and specialized applications. 6th edition*. John Wiley & Sons.

Fujito, N. T., Hanna, Z. R., Levy-Sakin, M., Bowie, R. C. K., Kwok, P.-Y., Dumbacher, J. P., & Wall, J. D. (2021). Genomic variation and recent population histories of Spotted (*Strix occidentalis*) and Barred (*Strix varia*) Owls. *Genome Biology and Evolution*, *13*(5), evab066. https://doi.org/10.1093/gbe/evab066

Gabriel, L., Brůna, T., Hoff, K. J., Ebel, M., Lomsadze, A., Borodovsky, M., & Stanke, M. (2023). BRAKER3: Fully automated genome annotation using RNA-seq and protein evidence with GeneMark-ETP, AUGUSTUS and TSEBRA. https://doi.org/10.1101/2023.06.10.544449

Guan, D., McCarthy, S. A., Wood, J., Howe, K., Wang, Y., & Durbin, R. (2020). Identifying and removing haplotypic duplication in primary genome assemblies. *Bioinformatics*, *36*(9), 2896–

2898. https://doi.org/10.1093/bioinformatics/btaa025

Gurevich, A., Saveliev, V., Vyahhi, N., & Tesler, G. (2013). QUAST: Quality assessment tool for genome assemblies. *Bioinformatics*, *29*(8), 1072–1075. https://doi.org/10.1093/bioinformatics/btt086

Hausknecht, R., Jacobs, S., Müller, J., Zink, R., Frey, H., Solheim, R., Vrezec, A., Kristin, A., Mihok, J., Kergalve, I., Saurola, P., & Kuehn, R. (2014). Phylogeographic analysis and genetic cluster recognition for the conservation of Ural Owls (*Strix uralensis*) in Europe. *Journal of Ornithology*, *155*(1), 121–134. https://doi.org/10.1007/s10336-013-0994-8

He, W., Yang, J., Jing, Y., Xu, L., Yu, K., & Fang, X. (2023). NGenomeSyn: An easy-to-use and flexible tool for publication-ready visualization of syntenic relationships across multiple genomes. *Bioinformatics*, *39*(3), btad121. https://doi.org/10.1093/bioinformatics/btad121

He, Z., Wilson, A., Rich, F., Kenwright, D., Stevens, A., Low, Y. S., & Thunders, M. (2023). Chromosomal instability and its effect on cell lines. *Cancer Reports*, *6*(6), e1822. https://doi.org/10.1002/cnr2.1822

Hoff, K. J., Lange, S., Lomsadze, A., Borodovsky, M., & Stanke, M. (2016). BRAKER1: Unsupervised RNA-Seq-Based Genome Annotation with GeneMark-ET and AUGUSTUS. *Bioinformatics*, *32*(5), 767–769. https://doi.org/10.1093/bioinformatics/btv661

Huang, N., & Li, H. (2023). compleasm: A faster and more accurate reimplementation of BUSCO. *Bioinformatics*, *39*(10), btad595. https://doi.org/10.1093/bioinformatics/btad595

Huerta-Cepas, J., Szklarczyk, D., Heller, D., Hernández-Plaza, A., Forslund, S. K., Cook, H., Mende, D. R., Letunic, I., Rattei, T., Jensen, L. J., von Mering, C., & Bork, P. (2019). eggNOG 5.0: A hierarchical, functionally and phylogenetically annotated orthology resource based on 5090 organisms and 2502 viruses. *Nucleic Acids Research*, *47*(D1), D309–D314. https://doi.org/10.1093/nar/gky1085

Hughes, P., Marshall, D., Reid, Y., Parkes, H., & Gelber, C. (2007). The costs of using unauthenticated, over-passaged cell lines: How much more data do we need? *BioTechniques*,

43(5), 575–586. https://doi.org/10.2144/000112598

Huntley, B., Green, R., Collingham, Y. C., & Willis, S. G. (2007). *A climatic atlas of european breeding birds*. Lynx ed.

IUCN. (2021). *Strix uralensis: BirdLife International: The IUCN Red List of Threatened Species 2021: e.T22689108A199908915* [Dataset]. https://doi.org/10.2305/IUCN.UK.2021-3.RLTS.T22689108A199908915.en

Jacques Dainat, Darío Hereñú, Dr. K. D. Murray, Ed Davis, Ivan Ugrin, Kathryn Crouch, LucileSol, Nuno Agostinho, pascal-git, Zachary Zollman, & tayyrov. (2024). *NBISweden/AGAT: AGAT-v1.4.1* (Version v1.4.1) [Computer software]. Zenodo. https://doi.org/10.5281/ZENODO.3552717

König, C., & Weick, F. (2009). *Owls of the World*. Yale University Press.

Kopij, G. (2011). *Population and range expansion of forest boreal owls*.

Kriventseva, E. V., Tegenfeldt, F., Petty, T. J., Waterhouse, R. M., Simão, F. A., Pozdnyakov, I. A., Ioannidis, P., & Zdobnov, E. M. (2015). OrthoDB v8: Update of the hierarchical catalog of orthologs and the underlying free software. *Nucleic Acids Research*, *43*(D1), D250–D256. https://doi.org/10.1093/nar/gku1220

Lehikoinen, A., Ranta, E., Pietiäinen, H., Byholm, P., Saurola, P., Valkama, J., Huitu, O., Henttonen, H., & Korpimäki, E. (2011). The impact of climate and cyclic food abundance on the timing of breeding and brood size in four boreal owl species. *Oecologia*, *165*(2), 349–355. https://doi.org/10.1007/s00442-010-1730-1

Li, H. (2013). *Aligning sequence reads, clone sequences and assembly contigs with BWA-MEM*. https://arxiv.org/abs/1303.3997

Li, H. (2018). Minimap2: Pairwise alignment for nucleotide sequences. *Bioinformatics*, *34*(18), 3094–3100. https://doi.org/10.1093/bioinformatics/bty191

Li, H., & Durbin, R. (2009). Fast and accurate short read alignment with Burrows–Wheeler

791 transform. *Bioinformatics*, *25*(14), 1754–1760. https://doi.org/10.1093/bioinformatics/btp324

792 Li, H., & Durbin, R. (2011). Inference of human population history from individual whole-
793 genome sequences. *Nature*, *475*(7357), 493–496. https://doi.org/10.1038/nature10231

794 Li, H., Handsaker, B., Wysoker, A., Fennell, T., Ruan, J., Homer, N., Marth, G., Abecasis, G.,
795 Durbin, R., & 1000 Genome Project Data Processing Subgroup. (2009). The Sequence
796 Alignment/Map format and SAMtools. *Bioinformatics*, *25*(16), 2078–2079.
797 https://doi.org/10.1093/bioinformatics/btp352

798 Manni, M., Berkeley, M. R., Seppey, M., Simão, F. A., & Zdobnov, E. M. (2021). BUSCO
799 update: Novel and streamlined workflows along with broader and deeper phylogenetic
800 coverage for scoring of eukaryotic, prokaryotic, and viral genomes. *Molecular Biology and*
801 *Evolution*, *38*(10), 4647–4654. https://doi.org/10.1093/molbev/msab199

802 Mead, D., Ogden, R., Meredith, A., Peniche, G., Smith, M., Corton, C., Oliver, K., Skelton, J.,
803 Betteridge, E., Doulcan, J., Holmes, N., Wright, V., Loose, M., Quail, M. A., McCarthy, S. A.,
804 Howe, K., Chow, W., Torrance, J., Collins, J., … Blaxter, M. (2021). The genome sequence of
805 the European golden eagle, *Aquila chrysaetos chrysaetos* Linnaeus 1758. *Wellcome Open*
806 *Research*, *6*, 112. https://doi.org/10.12688/wellcomeopenres.16631.1

807 Mikkola, H., & Willis, I. (1983). *Owls of Europe*. T & A D Poyser.
808 https://doi.org/10.5040/9781472597175

809 Miller, J. R., Delcher, A. L., Koren, S., Venter, E., Walenz, B. P., Brownley, A., Johnson, J., Li,
810 K., Mobarry, C., & Sutton, G. (2008). Aggressive assembly of pyrosequencing reads with
811 mates. *Bioinformatics*, *24*(24), 2818–2824. https://doi.org/10.1093/bioinformatics/btn548

812 Mooney, A., Ryder, O. A., Houck, M. L., Staerk, J., Conde, D. A., & Buckley, Y. M. (2023).
813 Maximizing the potential for living cell banks to contribute to global conservation priorities. *Zoo*
814 *Biology*, *42*(6), 697–708. https://doi.org/10.1002/zoo.21787

815 Odoemelam, E., Raghavan, N., Miller, A., Bridger, J. M., & Knight, M. (2009). Revised
816 karyotyping and gene mapping of the *Biomphalaria glabrata* embryonic (Bge) cell line.

International Journal for Parasitology, *39*(6), 675–681. https://doi.org/10.1016/j.ijpara.2008.11.011

Okonechnikov, K., Conesa, A., & García-Alcalde, F. (2016). Qualimap 2: Advanced multi-sample quality control for high-throughput sequencing data. *Bioinformatics*, *32*(2), 292–294. https://doi.org/10.1093/bioinformatics/btv566

O'Leary, N. A., Cox, E., Holmes, J. B., Anderson, W. R., Falk, R., Hem, V., Tsuchiya, M. T. N., Schuler, G. D., Zhang, X., Torcivia, J., Ketter, A., Breen, L., Cothran, J., Bajwa, H., Tinne, J., Meric, P. A., Hlavina, W., & Schneider, V. A. (2024). Exploring and retrieving sequence and metadata for species across the tree of life with NCBI Datasets. *Scientific Data*, *11*(1), 732. https://doi.org/10.1038/s41597-024-03571-y

Pichugin, A. M., Galkina, S. A., Potekhin, A. A., Punina, E. O., Rautian, M. S., & Rodionov, A. V. (2001). Estimation of the minimal size of chicken *Gallus gallus domesticus* microchromosomes via pulsed-field electrophoresis. *Russian Journal of Genetics*, *37*(5), 535–538. https://doi.org/10.1023/A:1016622816552

Poplin, R., Ruano-Rubio, V., DePristo, M. A., Fennell, T. J., Carneiro, M. O., Van Der Auwera, G. A., Kling, D. E., Gauthier, L. D., Levy-Moonshine, A., Roazen, D., Shakir, K., Thibault, J., Chandran, S., Whelan, C., Lek, M., Gabriel, S., Daly, M. J., Neale, B., MacArthur, D. G., & Banks, E. (2017). *Scaling accurate genetic variant discovery to tens of thousands of samples*. https://doi.org/10.1101/201178

Quinlan, A. R., & Hall, I. M. (2010). BEDTools: A flexible suite of utilities for comparing genomic features. *Bioinformatics*, *26*(6), 841–842. https://doi.org/10.1093/bioinformatics/btq033

Ranallo-Benavidez, T. R., Jaron, K. S., & Schatz, M. C. (2020). GenomeScope 2.0 and Smudgeplot for reference-free profiling of polyploid genomes. *Nature Communications*, *11*(1), 1432. https://doi.org/10.1038/s41467-020-14998-3

Ratnasingham, S., & Hebert, P. D. N. (2007). BOLD: The Barcode of Life Data System (http://www.barcodinglife.org). *Molecular Ecology Notes*, *7*(3), 355–364.

https://doi.org/10.1111/j.1471-8286.2007.01678.x

Raxworthy, M. (1987). Animal cell culture: A practical approach. *Biochemical Education*, *15*(1), 53. https://doi.org/10.1016/0307-4412(87)90173-7

Rebholz, W. E. R., Boer, L. E. M. D., Sasaki, M., Belterman, R. H. R., & Nishida-Umehara, C. (1993). The chromosomal phylogeny of owls (Strigiformes) and new karyotypes of seven species. *CYTOLOGIA*, *58*(4), 403–416. https://doi.org/10.1508/cytologia.58.403

Rhie, A., Walenz, B. P., Koren, S., & Phillippy, A. M. (2020). Merqury: Reference-free quality, completeness, and phasing assessment for genome assemblies. *Genome Biology*, *21*(1), 245. https://doi.org/10.1186/s13059-020-02134-9

Ryder, O. A., & Onuma, M. (2018). Viable cell culture banking for biodiversity characterization and conservation. *Annual Review of Animal Biosciences*, *6*(1), 83–98. https://doi.org/10.1146/annurev-animal-030117-014556

Scherzinger, W. (2006). Die Wiederbegründung des Habichtskauz-Vorkommens Strix uralensis im Böhmerwald. *Ornithologischer Anzeiger*, *45*(2/3), 97–156.

Scope, A., Schwendenwein, I., Stanclova, G., Vobornik, A., & Zink, R. (2016). Exploratory plasma biochemistry reference intervals for Ural Owls (*Strix uralensis*, Pallas 1771) from the Austrian reintroduction project.. *Journal of Zoo and Wildlife Medicine*, *47*(2), 486–492. https://doi.org/10.1638/2015-0200.1

Shen, W., Le, S., Li, Y., & Hu, F. (2016). SeqKit: A cross-platform and ultrafast toolkit for FASTA/Q file manipulation. *PLOS ONE*, *11*(10), e0163962. https://doi.org/10.1371/journal.pone.0163962

Shen, W., Sipos, B., & Zhao, L. (2024). SeqKit2: A Swiss army knife for sequence and alignment processing. *iMeta*, *3*(3), e191. https://doi.org/10.1002/imt2.191

Smith, J., Bruley, C. K., Paton, I. R., Dunn, I., Jones, C. T., Windsor, D., Morrice, D. R., Law, A. S., Masabanda, J., Sazanov, A., Waddington, D., Fries, R., & Burt, D. W. (2000).

Differences in gene density on chicken macrochromosomes and microchromosomes. *Animal Genetics*, *31*(2), 96–103. https://doi.org/10.1046/j.1365-2052.2000.00565.x

Song, J., Hua, S., Song, K., & Zhang, Y. (2007). Culture, characteristics and chromosome complement of Siberian tiger fibroblasts for nuclear transfer. *In Vitro Cellular & Developmental Biology - Animal*, *43*(7), 203–209. https://doi.org/10.1007/s11626-007-9043-3

Soorae, P. S. (2011). *Global re-introduction perspectives, 2011: More case studies from around the globe*. IUCN/SSC Re-introduction Specialist Group & Environment Agency - Abu Dhabi.

Storer, J., Hubley, R., Rosen, J., Wheeler, T. J., & Smit, A. F. (2021). The Dfam community resource of transposable element families, sequence models, and genome annotations. *Mobile DNA*, *12*(1), 2. https://doi.org/10.1186/s13100-020-00230-y

Supek, F., Bošnjak, M., Škunca, N., & Šmuc, T. (2011). REVIGO summarizes and visualizes long lists of gene ontology terms. *PLoS ONE*, *6*(7), e21800. https://doi.org/10.1371/journal.pone.0021800

Takagi, N., & Sasaki, M. (1974). A phylogenetic study of bird karyotypes. *Chromosoma*, *46*(1), 91–120. https://doi.org/10.1007/BF00332341

Tarailo-Graovac, M., & Chen, N. (2009). Using RepeatMasker to identify repetitive elements in genomic sequences. *Current Protocols in Bioinformatics*, *25*(1). https://doi.org/10.1002/0471250953.bi0410s25

Terhorst, J., Kamm, J. A., & Song, Y. S. (2017). Robust and scalable inference of population history from hundreds of unphased whole genomes. *Nature Genetics*, *49*(2), 303–309. https://doi.org/10.1038/ng.3748

Uliano-Silva, M., Ferreira, J. G. R. N., Krasheninnikova, K., Darwin Tree of Life Consortium, Blaxter, M., Mieszkowska, N., Hall, N., Holland, P., Durbin, R., Richards, T., Kersey, P., Hollingsworth, P., Wilson, W., Twyford, A., Gaya, E., Lawniczak, M., Lewis, O., Broad, G., Martin, F., … McCarthy, S. A. (2023). MitoHiFi: A python pipeline for mitochondrial genome

894 assembly from PacBio high fidelity reads. *BMC Bioinformatics*, *24*(1), 288.
895 https://doi.org/10.1186/s12859-023-05385-y

896 Uliano-Silva, M., Gabriel R. N. Ferreira, J., Krasheninnikova, K., Darwin Tree of Life
897 Consortium, Formenti, G., Abueg, L., Torrance, J., Myers, E. W., Durbin, R., Blaxter, M., &
898 McCarthy, S. A. (2022). MitoHiFi: A python pipeline for mitochondrial genome assembly from
899 PacBio High Fidelity reads. https://doi.org/10.1101/2022.12.23.521667

900 Vrezec, A. (2009). Melanism and plumage variation in macroura Ural Owl. *Dutch Birding*,
901 *31*(3), 159–170.

902 Wenger, S. L., Senft, J. R., Sargent, L. M., Bamezai, R., Bairwa, N., & Grant, S. G. (2005).
903 Comparison of established cell lines at different passages by karyotype and comparative
904 genomic hybridization. *Bioscience Reports*, *24*(6), 631–639. https://doi.org/10.1007/s10540-
905 005-2797-5

906 Wood, D. E., Lu, J., & Langmead, B. (2019). Improved metagenomic analysis with Kraken 2.
907 *Genome Biology*, *20*(1), 257. https://doi.org/10.1186/s13059-019-1891-0

908 Yamada, K., Nishida-Umehara, C., & Matsuda, Y. (2004). A new family of satellite DNA
909 sequences as a major component of centromeric heterochromatin in owls (Strigiformes).
910 *Chromosoma*, *112*(6), 277–287. https://doi.org/10.1007/s00412-003-0267-z